Quaternary Science Reviews 230 (2020) 106065

Contents lists available at ScienceDirect

Quaternary Science Reviews

journal homepage: www.elsevier.com/locate/quascirev

Invited Review

Deep Pacific storage of respired carbon during the last ice age: Perspectives from bottom water oxygen reconstructions

A.W. Jacobel [a, *, 1], R.F. Anderson [a, b], S.L. Jaccard [c], J.F. McManus [a, b], F.J. Pavia [a, b], G. Winckler [a, b]

[a] Lamont-Doherty Earth Observatory, Palisades, NY, USA
[b] Department of Earth and Environmental Sciences, Columbia University, New York, NY, USA
[c] Institute of Geological Sciences and Oeschger Center for Climate Change Research, University of Bern, Bern, Switzerland

ARTICLE INFO

Article history:
Received 8 July 2019
Received in revised form
8 November 2019
Accepted 8 November 2019
Available online 26 November 2019

Keywords:
Carbon
Oxygen
Geochemical archives
Paleoclimate
Ocean Drilling Program
Ocean carbon storage

ABSTRACT

Reconstructions of past changes in dissolved oxygen concentrations in the abyssal ocean are of interest to paleoceanographers because of their potential to help characterize and quantify the transfer of carbon between the atmosphere and the deep ocean. This potential, derived from the stoichiometric relationship between oxygen consumption and the regeneration of organic matter, has recently been expanded by compilations of core top observations for two proxies: the $\delta^{13}C$ gradient between coeval infaunal and epifaunal benthic foraminifera ($\Delta\delta^{13}C$), and biomarker preservation. Here, we review these newer proxies, and the more established redox proxy authigenic uranium (aU), to critically evaluate our understanding of the controls on proxy signal production and preservation. We locate our work in the equatorial Pacific, presenting both new data and a compilation of existing records from thirty-two sediment cores to draw semi-quantitative conclusions about bottom water oxygen and respired carbon concentrations over the last glacial period. We find that the biogeochemical limitations on these proxies may be more substantial than previously appreciated, and therefore suggest several best-practice recommendations for their application. Despite the recognized data limitations, the compilation identifies the glacial Pacific Ocean as a dominant sink for CO_2 at all depths below the modern oxygen minimum zone. Our review emphasizes the importance of multiproxy reconstructions, informed by site-specific records of paleoproductivity, in drawing coherent, internally consistent conclusions about glacial ocean oxygenation and carbon storage.

1. Introduction

The partitioning of carbon between the atmosphere, oceans, biosphere, and shallow lithosphere is one of the most fundamental controls on Earth's climate system. At present, the most important carbon exchange between the ocean and atmosphere occurs as anthropogenic CO_2 equilibrates in surface water, on average drawing CO_2 into the global oceans and leading to the acidification of shallow waters. On interannual and longer timescales, ocean physics and biogeochemical transformations act to draw CO_2 from the surface ocean deep into the ocean's interior though a combination of processes including cooling-induced increases in CO_2 solubility, enhanced ocean alkalinity, strengthened/increased efficiency of the ocean's soft-tissue biological pump, enhanced water mass stratification, and inhibited air-sea exchange (including through limited surface residence time and/or expanded sea ice cover) (Archer et al., 2000; Sigman and Boyle, 2000). Reconstructions of natural variation in the climate system's allocation of carbon can provide insights into the nature, relative importance of, and interplay between the various mechanisms and feedbacks involved in ocean carbon storage and release. Using past changes in the climate system as experimental realizations to investigate the consequences of carbon export for deep carbon storage and oxygen levels is thus critical for helping improve predictions of how the oceans will respond to anthropogenic climate forcing beyond the next few decades.

Because of the stoichiometric relationship between respired

* Corresponding author.
E-mail address: jacobel@brown.edu (A.W. Jacobel).
[1] Now at: Institute at Brown for Environment and Society, and the Department of Earth, Environmental, and Planetary Sciences, Brown University, Providence, RI, USA.

https://doi.org/10.1016/j.quascirev.2019.106065
0277-3791/

carbon accumulation and the removal of oxygen through bacterial respiration, proxy data reflecting bottom water oxygen (BWO) concentrations are of value in understanding deep ocean carbon storage. In the early 90's Boyle recognized the potential significance of these data when he added paleo-O_2 to his proxy "wish list" (Boyle, 1990) for solving the problems of Quaternary deepwater paleoceanography. One of the advantages of using O_2 over seemingly more direct measures of oceanic respired carbon such as benthic foraminifera $\delta^{13}C$, is that during air-sea exchange oxygen equilibrates an order of magnitude faster than CO_2 (Broecker and Peng, 1974), more effectively resetting its saturation state, before surface waters are downwelled to form intermediate-and deep water masses. In practice, this means that BWO can be interpreted more directly as indicative of the integrated water mass respiration history since the time of most recent ventilation, avoiding some of the problems associated with inherited air-sea $\delta^{13}C$ signatures, and terrestrial biosphere variations in $\delta^{13}C$. Some oxygen undersaturation has been suggested for the 'average' surface waters that give rise to Weddell Sea deep waters but these effects are likely small (~4%) (A. L. Gordon and Huber, 1990) and disequilibrium would lead to, if anything, an underestimate of respiratory CO_2 storage in deep waters (discussion in Anderson et al., 2019; Ito and Follows, 2013). An additional advantage of using BWO to reconstruct respired carbon storage is that on the basin scale it is largely insensitive to hydrothermal CO_2 input. This feature permits differentiation of the atmosphere-ocean partitioning of carbon via the biological pump, and the submarine injection of dissolved inorganic carbon. Work suggesting that volcanic sources of CO_2 may have been important contributor to the ^{14}C signature of deglacial carbon release (Stott and Timmermann, 2011) makes parsing these contributions particularly important, and BWO reconstructions provide the opportunity to do so.

Despite the advantages of using BWO to reconstruct respired carbon storage, progress towards its utilization has been slow, largely because developing a quantitative paleo proxy for dissolved O_2 has proven to be a challenge. Recently, the carbon isotope gradient between coeval epifaunal and infaunal benthic foraminifera ($\Delta\delta^{13}C$), was empirically calibrated to BWO concentrations in a study by Hoogakker et al. (2015), building on original work by McCorkle and co-authors (1985). In parallel, a new study employed the preserved sedimentary abundance of biomarkers as a semi-quantitative proxy for dissolved O_2 (Anderson et al., 2019). These approaches add to the classical literature on redox-sensitive metal enrichments in sediments (*e.g.*: Mn, Mo, Re, and U) that have been used as qualitative proxies for bottom water redox state. Records of authigenic uranium (aU) are particularly abundant, and the co-location of these records at sites where the newer proxies have also been measured has motivated us to synthesize and review these proxy systems. We focus our review on the equatorial Pacific for two key reasons. First, existing studies that have endeavored to assess past changes in carbon storage have consistently demonstrated the importance of the Pacific Ocean (*e.g.*: Allen et al., 2015; Anderson et al., 2019; Bradtmiller et al., 2010; Duchamp-Alphonse et al., 2018; Hoogakker et al., 2018; Jaccard and Galbraith, 2013, 2012; Jaccard et al., 2009; Jacobel et al., 2017; Ronge et al., 2016; Umling and Thunell, 2018; Wagner and Hendy, 2017). This work has conclusively resolved previously conflicting interpretations (*e.g.*: Broecker and Clark, 2010; Broecker et al., 2008) that arose from studies seeking to establish changes in water mass ventilation ages as indicative of carbon storage. Indeed, many obstacles to a straightforward implementation of the ventilation age approach have been identified (*e.g.*: Broecker and Clark, 2011; Mekik, 2014; Rafter et al., 2018; Ronge et al., 2016; Stott and Timmermann, 2011; Zhao and Keigwin, 2018), suggesting that reconstructions of carbon storage and oxygen levels are a more promising way to assess the atmosphere-ocean partitioning of carbon. Having qualitatively established that the Pacific Ocean is an important site for glacial carbon storage, recent efforts have turned to addressing the twin questions of how much additional carbon was stored in the ocean interior, and in which water masses specifically. The equatorial Pacific is a good testing ground for answering these questions because of the large number of proxy reconstructions, spanning a range of depths that reflect different water masses and source locations (Fig. 1). The water masses covered by these proxy reconstructions include North Pacific Intermediate Water (NPIW), North Pacific Deep Water (NPDW), Antarctic Intermediate Water (AAIW), and Lower Circumpolar Deep Water (LCDW), which together constitute almost all of the subsurface water in the Pacific Ocean.

Here, we combine new aU and $\Delta\delta^{13}C$ data with previously published results to provide a picture of glacial carbon storage and Pacific water mass structure that is internally consistent. We begin with an overview of the three most promising proxies for BWO: aU, $\Delta\delta^{13}C$, and selective biomarker preservation. Next, we compare records of these proxies from ODP Site 1240 where all three have been measured. The co-registration of these proxies permits a direct intra-core assessment that is immune from limitations that might otherwise arise in comparisons of data from multiple cores, due to confounding variables including different sedimentation rates, age models, and export production histories. Having drawn new conclusions about the respective advantages and limitations of the proxies at a single site, we then investigate the multiproxy records of thirty-two sediment cores (Table 1) spanning the equatorial Pacific. Where possible we extend our proxy comparisons over the last 150 ka, in order to gain additional insight into the variable controls on proxy production and preservation, but otherwise focus our paleoceanographic interpretations on the last 30 ka, the time period over which we have the greatest spatial and water mass depth coverage in our compilation. Inter-comparison of these records, grouped by proxy, allows for critical evaluation of the relative strengths and limitations of existing BWO proxies. We use our compilation to summarize the state of our knowledge of deep Pacific glacial oxygen and respired carbon storage, suggest best practices for future proxy applications and record interpretation, and propose promising directions for future research.

2. Approaches

2.1. aU

Uranium is present in oxygenated seawater in the soluble form U(VI), predominantly as calcium uranyl carbonate complexes (Dong and Brooks, 2006; Endrizzi and Rao, 2014). Although particulate U is found in the upper ocean in association with lithogenic sediment, organic carbon, and foraminiferal calcite (Anderson, 1982), the primary mechanism of U removal from the ocean is through its authigenic precipitation in reducing porewaters (Klinkhammer and Palmer, 1991; J. McManus et al., 2005). Indeed, in open ocean settings, U associated with organic carbon is typically remobilized and recycled before reaching the seafloor (Zheng et al., 2002a) (Supplementary Note 1), and the contribution from sinking foraminifera is negligible (~0.012–0.036 ppm) (Russell et al., 2004). At the seafloor, U diffuses from seawater into the sediment and is authigenically precipitated from porewaters under reducing conditions that occur below the depth where sediments become suboxic. The exact mechanism for the reduction of U(VI) to U(IV) remains uncertain, but the observation that U reduction occurs near the reduction potential associated with conversion of Fe(III) to Fe(II) suggests that it may be mediated by iron-reducing microbes that can substitute U as an electron acceptor (Finneran et al., 2002;

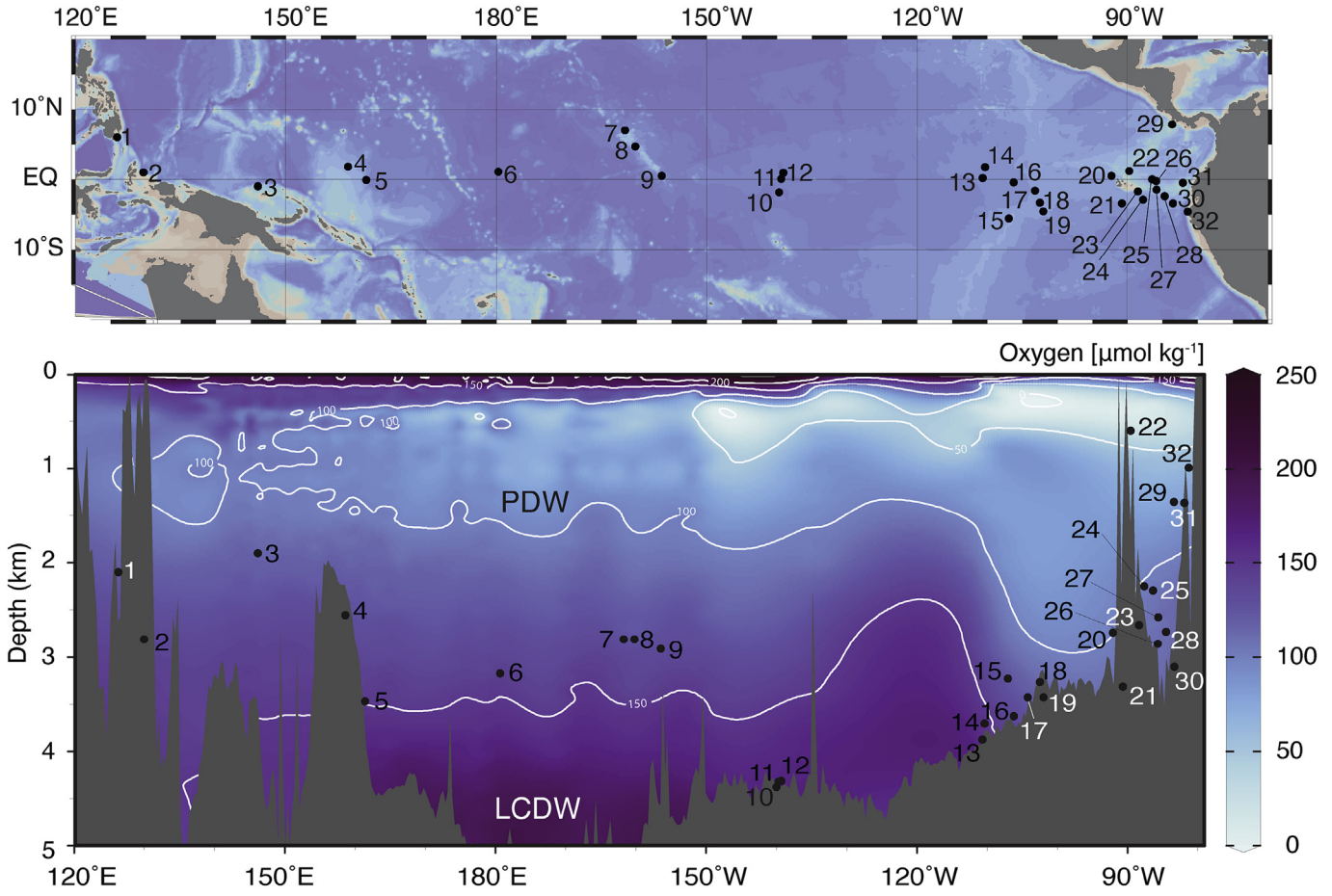

Fig. 1. Map of Study Sites. Map of the equatorial Pacific Ocean with study sites numbered from west to east. A) Map view. B) Cross sectional view with colored contours indicating modern oxygen concentrations in µmol kg−1. Site numbers correspond to the location and proxy information in Table 1. Figure made using Ocean Data View software (Schlitzer, 2016) with basemap oxygen data from (Suzuki et al., 2013).

J. McManus et al., 2005). As the reduction and precipitation of U proceeds, it creates a concentration gradient between the sediment-water interface and the depth of U reduction in the sediments, driving a diffusive flux into the sediment and generating intervals of high sedimentary aU. In the present study, aU is quantified using the established activity ratio between lithogenic ^{238}U and ^{232}Th for the Pacific (0.7 ± 0.1) (Henderson, 2003). This allows for the subtraction of lithogenic U from the total U where

$$^{238}U_{auth} = {}^{238}U_{total} - 0.7 * {}^{232}Th_{meas}$$

Because aU is precipitated from dissolved U in the porewaters, it is the porewater redox state that determines its solubility. Indeed, modern accumulations of sedimentary aU are found in regions where BWO concentrations are oxic, but where the high flux of organic material to the seafloor creates reducing conditions that lead to authigenic U precipitation via anaerobic microbial respiration following the depletion of free molecular oxygen (J. McManus et al., 2005). The significance of this observation is twofold. First, the presence or absence of aU in the sedimentary record does not put quantitative bounds on the concentration of oxygen present in bottom water. Second, the precipitation of aU can be fostered by an increase in the sedimentary flux and associated respiration of organic matter, a decrease in the oxygen concentration of bottom waters, or a combination of both processes (Fig. 2). This means that the interpretation of aU as a proxy for BWO requires detailed understanding of the co-occurring flux of labile organic carbon to the site. Common proxies for this carbon flux include ^{230}Th-normalized fluxes of biogenic barium (Ba_{xs}) (François et al., 1995; Hernandez-Sanchez et al., 2011) or biogenic opal (Leinen et al., 1986), which are thought to be more resistant to water column/post-depositional alteration (especially by variable BWO) than organic proxies such as the abundance of algal lipid biomarkers *e.g.:* $C_{37:total}$, which will be discussed in Section 2.3. Here, we use Ba_{xs} as a proxy for integrated organic carbon rain at ODP Site 1240, but also utilize a record of opal flux from Hayes et al. (2011) in an effort to minimize the effect of their independent production and preservation biases on our interpretations.

Because of the sensitivity of U to the presence of oxygen, post depositional alteration of aU ("burndown") is not uncommon and has been studied extensively in basins characterized by large variations in bottom-water oxygenation and/or sediment accumulation (Colley and Thomson, 1985; Colley et al., 1989; Shaw et al., 1994; Thomson et al., 1996). The diagenetic behavior of aU can vary significantly depending on the depositional environment, timeline of initial aU precipitation, and exposure to oxygen (or a reduction in the rain of organic carbon (J. McManus et al., 2005)). Complete dissolution and removal of aU (Zheng et al., 2002b), partial dissolution (Jacobel et al., 2017), and dissolution and downcore reprecipitation (Colley and Thomson, 1985) have been observed and must be screened for carefully. In the context of qualitatively interpreting aU records, the first issue is of greatest concern and therefore in this study we highlight records from cores

Table 1
Core summary.

Site #	Core Name	Latitude (DDS)	Longitude (DDS)	Depth (km)	Reference(s)
1	MD98-2181	6.0	126.0	2.1	Broecker et al. (2004)
2	MD01-2386	1.0	130.0	2.8	Broecker et al. (2008)
3	MD97-2138	−1.3	146.0	1.9	(Bradtmiller et al., 2006; Broecker et al., 2004)
4	RC17-177	1.5	159.0	2.6	Bradtmiller et al. (2006)
5	MW91-9 GG 48	0.0	161.0	3.4	Bradtmiller et al. (2006)
6	V28-203	1.0	−179.3	3.2	Bradtmiller et al. (2006)
7	ML1208-37BB	7.0	−161.6	2.8	Jacobel et al. (2017)
8	ML1208-31BB	4.7	−160.1	2.8	Jacobel et al. (2017)
9	ML1208-17 PC	0.5	−156.4	2.9	Jacobel et al. (2017)
10	TTN013-PC18	−1.8	−139.7	4.4	(Anderson et al., 2019; Bradtmiller et al., 2010, 2016; Broecker and Clark, 2010)
11	TTN013-PC72	0.1	−139.4	4.3	Anderson et al. (2019)
12	MANOP C	0.9	−139.0	4.3	Prahl et al. (1989b)
13	ODP 849	0.2	−110.6	3.9	(Pichat et al., 2014; Winckler et al., 2008)
14	KNR 73 4 PC	1.8	−110.3	3.7	Thiagarajan and J. F. McManus (2019)
15	V21-40	−5.5	−106.8	3.2	Bradtmiller et al. (2006)
16	KNR 73 3 PC	−0.4	−106.2	3.6	Thiagarajan and J. F. McManus (2019)
17	RC13-114	−1.7	−103.6	3.4	Bradtmiller et al. (2006)
18	PLDS 7G	−3.3	−102.5	3.3	Thiagarajan and J. F. McManus (2019)
19	VNTR01 10 GC	−4.5	−102.0	3.4	Thiagarajan and J. F. McManus (2019)
20	TR163-23	0.4	−92.2	2.7	Umling and Thunell (2018)
21	ODP 846	−3.4	−90.8	3.3	This study, (Herbert et al., 2010)
22	VM21-30 PC	1.2	−89.7	0.6	(Anderson et al., 2019; Bradtmiller et al., 2006; Koutavas and Sachs, 2008)
23	TR163-25	−1.7	−88.5	2.7	Hoogakker et al. (2018)
24	RC13-140	−2.9	−87.8	2.2	Bradtmiller et al. (2010)
25	ODP 1240	0.0	−86.5	2.3	This study, (Calvo et al., 2011; de la Fuente et al., 2015)
26	MV1014-17JC	−0.2	−85.9	2.8	Loveley et al. (2017)
27	RC11-238	−1.5	−85.8	2.6	(Anderson et al., 2019; Bradtmiller et al., 2006; Koutavas and Sachs, 2008)
28	VM19-28 PC	−2.4	−84.7	2.7	(Anderson et al., 2019; Koutavas and Sachs, 2008)
29	ODP 1242	7.9	−83.6	1.4	Hoogakker et al. (2018)
30	VM19-30 PC	−3.4	−83.5	3.1	(Anderson et al., 2019; Bradtmiller et al., 2006; Koutavas and Sachs, 2008)
31	VM19-27 PC	−0.5	−82.1	1.4	(Anderson et al., 2019; Koutavas and Sachs, 2008)
32	CDH 26	−4.0	−81.3	1.0	Bova et al. (2018)

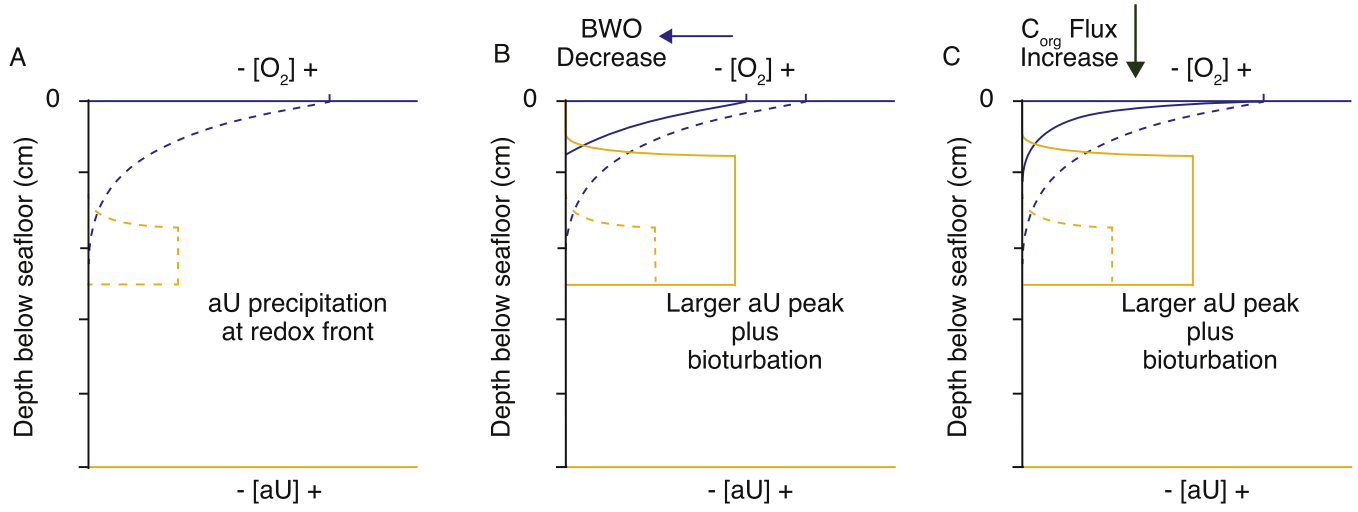

Fig. 2. Schematic of aU Responses to Redox Changes. Panel A depicts a baseline scenario where BWO and C_{org} flux combine to create porewater oxygen conditions (dashed blue line) conducive to the precipitation of solid phase aU (dashed gold line). In Panel B the BWO is decreased, maintaining the slope of the oxicline (solid blue line) but shoaling the depth of the redox front and accordingly, the depth of aU precipitation (solid gold line). Assuming that other factors, including diffusivity (K) and mass accumulation rate (MAR), are held constant, the flux of dissolved U into sediments (F) varies inversely with the depth below the sediment water interface of U precipitation (∂z), according to $F = K(\partial C/\partial z)$, where ∂C is the difference in U concentration between bottom water and at the depth of U precipitation (effectively zero). Therefore, the concentration of aU in the sediments, which is equivalent to F/MAR, will increase as the depth of U precipitation decreases (dashed gold line). In Panel C, BWO conditions are the same as in A, but the C_{org} flux is increased, resulting in a steepening of the oxicline (solid blue line) and shoaling the depth of aU precipitation (solid gold line). As in B, the original aU peak is enhanced. Bioturbation smooths the new and original peaks together. Note that the sharp edges of the peaks reflect an idealized case at the time of deposition.

with glacial sedimentation rates greater than 3 cm ka^{-1}, a delineation based on the observation that sediments accumulation at rates lower than 2 cm ka^{-1} appear most susceptible to diagenetic aU loss (Mangini et al., 2001) upon re-exposure to O_2. Additionally, we exercise caution when interpreting abrupt changes in the abundance of aU, as these transitions may be associated with "burndown layers" (Crusius and Thomson, 2000), rather than truly abrupt changes in the sedimentary redox state reflecting equally abrupt paleoceanographic changes.

2.2. $\Delta\delta^{13}C$

McCorkle and co-authors were the first to propose the theoretical underpinnings of a benthic foraminifera-based carbon isotope proxy to quantitatively reconstruct BWO concentrations (McCorkle and Emerson, 1988; McCorkle et al., 1985, 1990, 1997). The proxy made use of the observed relationship between the respiratory release of isotopically light dissolved inorganic carbon and the concomitant consumption of oxygen in sedimentary porewaters (Fig. 3). McCorkle et al. proposed that if the carbon isotope gradient between oxic bottom water and the sedimentary oxic-anoxic boundary could be captured by epifaunal and infaunal benthic foraminifera then the BWO concentration could be quantitatively reconstructed. For almost 20 years proxy development awaited a core top calibration. Hoogakker et al. (2015) used core top, bottom water, and pore water observations of $\delta^{13}C$ to quantitatively relate the $\Delta\delta^{13}C$ gradient between surface sediments and the sedimentary oxic-anoxic boundary to BWO concentrations overlying their study sites. Their calibration equation directly relates BWO concentrations and the $\Delta\delta^{13}C$ between epifaunal *Cibicidoides wuellerstorfi* and infaunal *Globobulimina spp.*, using a robust linear relationship where $\Delta\delta^{13}C = 0.0064 * [O_2] + 0.555$ for oxygen concentrations ($\Delta\delta^{13}C$) between 55 (0.91‰) and 235 μmol kg^{-1} (2.06‰). The calibration of Hoogakker and colleagues has since yielded records of BWO at 6 sites in the Atlantic (Gottschalk et al., 2016; Hoogakker et al., 2015, 2016) and Pacific Oceans (Hoogakker et al., 2018; Umling and Thunell, 2018), allowing for the first quantitative estimates of respired carbon storage in the glacial ocean based on the stoichiometric relationship between BWO and respired carbon concentrations.

The $\Delta\delta^{13}C$ proxy relies on the assumption that the respiratory release of low $\delta^{13}C$ carbon (or 'isotopically light' carbon) is systematically correlated with a stoichiometric reduction in porewater oxygen concentrations. If isotopically light carbon not associated with oxic respiration is added to the porewaters from which *Globobulimina spp.* calcifies, then the theoretical relationship outlined above will break down. The anaerobic addition of isotopically light carbon will create a $\Delta\delta^{13}C$ gradient that is larger than the one that could be attributed exclusively to oxic respiration and thus the reconstructed BWO concentrations will be too high (green lines in Fig. 3). Indeed, McCorkle and co-authors (1988) warned about the potential for sulfate reduction and subsequent diffusion of isotopically light carbon to obscure the theoretical relationship between the respiratory consumption of oxygen and the carbon isotope gradient between benthic foraminifera. However, only recently has our understanding of infaunal benthic foraminifera physiology advanced sufficiently to understand the additional impact of *in-situ* anaerobic processes on these organisms. In sections 5.1 and 5.2.2 we summarize recent evidence that *Globobulimina spp.* denitrify, and discuss the attendant implications for the use of $\Delta\delta^{13}C$ as a BWO proxy.

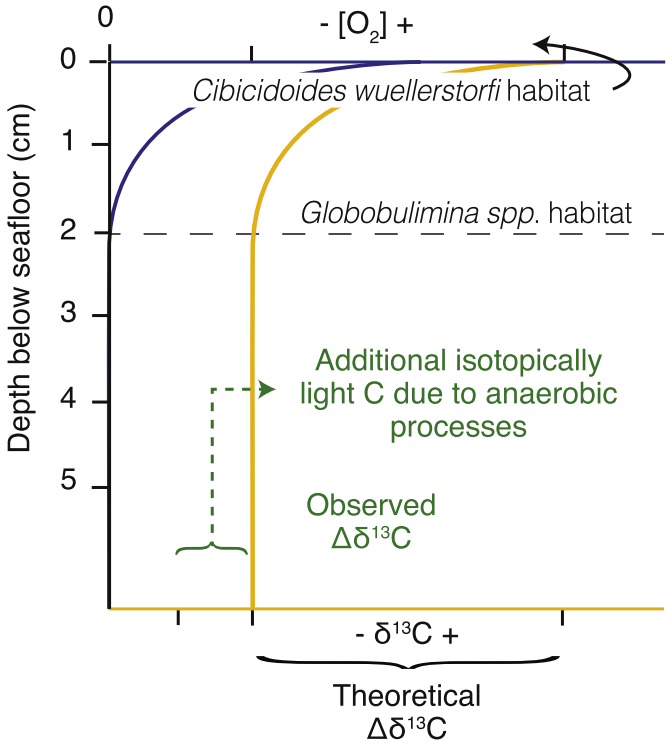

Fig. 3. Schematic of the $\Delta\delta^{13}C$ Proxy. *C. wuellerstorfi* live at the sediment-water interface (0 cm below seafloor) and their tests reflect the local carbon isotope composition of deep waters. Deeper in the sediment, light carbon is released (gold line, lower x axis) in proportion to the amount of oxygen consumed (blue line, upper x axis). In this theoretical schematic *Globobulimina spp.* live at the sedimentary porewater oxic/anoxic boundary at depth within the sediment. The carbon isotopic composition of their tests can be subtracted from that of the *C. wuellerstorfi* to yield a $\Delta\delta^{13}C$ value which has been observationally related to BWO concentrations. Green lines indicate the influence of additional isotopically light carbon from anaerobic respiration in *Globobulimina spp.*

2.3. Biomarker preservation

The sedimentary abundance of selected organic biomarkers is a frequently used proxy for marine export productivity (*e.g.*: Hinrichs et al., 1999; Prahl et al., 2000; Sachs and Anderson, 2005; Ternois et al., 2001; Venti et al., 2017) including in the equatorial Pacific Ocean (*e.g.*: Bova et al., 2018; Calvo et al., 2011). Among the most commonly used proxies is the total abundance of the long-chain unsaturated C_{37} ketones ($C_{37:total}$), which are produced by a few species of single-celled haptophyte algae, including coccolithophorid algae, in the ocean's photic zone (Herbert, 2003). The concentration (or preferably flux) of these alkenones measured in marine sediments has been related to the overlying water column productivity (*e.g.*: Prahl et al., 2000).

It has long been recognized that exposure to dissolved oxygen is the critical variable determining the preservation of organic compounds in marine sediments (Hartnett et al., 1998), one reason traditional metrics of productivity like percent total organic carbon (TOC) have fallen out of favor in oxic sedimentary environments. Recent work by Rodrigo-Gámiz et al. (2016) provides a quantitative perspective on this finding, presenting results from a ~20 km transect of sites in the Arabian Sea reflecting a range of BWO concentrations from 3 to 77 μmol kg^{-1}. Data from these sites show strong linear relationships between increased residence time in the oxic zone of the sediment and decreased concentrations of the di- and tri-unsaturated C_{37} ketones ($R^2 = 0.98$ and 0.94 respectively). The results of Rodrigo-Gámiz and co-authors suggest two possible interpretations of $C_{37:total}$ values: 1) where BWO concentrations can be shown to have remained approximately constant over time, large variations in $C_{37:total}$ can be interpreted as a change in productivity. 2) Where productivity can be shown to have remained approximately constant over time, large variations in $C_{37:total}$ can be interpreted as indicative of changes in BWO (Anderson et al., 2019). In this study, following the work of (Anderson et al., 2019), we use strong evidence of lower LGM export production relative to Holocene levels (Costa et al., 2017; Winckler et al., 2016) to interpret large deglacial changes in $C_{37:total}$ as indicative of threshold changes in BWO.

3. Methods

3.1. Data compilation

Data from thirty-two sediment core sites spanning from 126.0°E to 81.3°W were compiled for this study (Table 1, Fig. 1A). The cores span a range of water depths from 0.6 to 4.4 km and intersect water masses including LCDW, and PDW (Fig. 1B). Unless otherwise noted, all data are presented on the age model original to their publication.

3.2. New core sites

We present new data from two sites in the eastern equatorial Pacific Ocean (EEP), ODP Site 1240 (0.0°N, 86.4°W; 2.9 km water depth) and ODP Site 846 (3.0°S, 90.8°W; 3.3 km water depth) (Fig. 1A, sites 25 and 21 respectively). These sites were chosen for their potential to allow for reconstructions of paleo NPDW and LCDW water mass geochemistry and because both have been previously investigated (*e.g.*: Calvo et al., 2011; Herbert et al., 2010; de la Fuente et al., 2015) providing useful ancillary constraints. Additionally, core logs indicated that both sites were consistently populated by *Globobulimina spp*., providing the opportunity to reconstruct and evaluate new $\Delta\delta^{13}C$ proxy records.

ODP Site 1240 lies on the northern flank of the Carnegie Ridge in the Panama Basin (east of the Galapagos Islands) and at 2.9 km is presently bathed by a mixture of Pacific Deep Water entering the basin from the north, and southern-sourced LCDW (Mix et al., 2003) (Fig. 1B). At ODP Site 1240 modern oxygen concentrations at depth amount to ~110 μmol kg^{-1} (Suzuki et al., 2013) and the $\delta^{13}C$ of the nearest-neighbor bottom water measurement (8.0°S, 85.84°W; 3.0 km) suggests values in the range of −0.10‰ (Schmittner et al., 2017). The actual bottom water $\delta^{13}C$ value at ODP Site 1240 is almost certainly lower than the nearest-neighbor data point due to the comparison site's location significantly further south of the equatorial upwelling region and outside of the Panama Basin's enclosed circulation. For ODP Site 1240 we adopt the adjusted age model of Rippert et al. (2017), which used radiocarbon dates, and $\delta^{18}O$ data from *C. wuellerstorfi* to refine the previous model of (Pena et al., 2008). This age model yields sedimentation rates in the range of ~15 cm ka^{-1} during the Holocene and ~20 cm ka^{-1} at the LGM.

ODP Site 846 is located on the southern flank of the Carnegie Ridge and is bathed by a relatively higher proportion of LCDW as a consequence of its location outside of the Panama Basin and its greater depth (Mayer et al., 1992). At present, oxygen concentrations at the depth of ODP Site 846 are ~135 μmol kg^{-1} (Suzuki et al., 2013), higher than at ODP Site 1240 and most likely a consequence of lower productivity outside of the Panama Basin and the higher proportion of well-ventilated, southern-sourced water at this deeper site. The nearest-neighbor water column $\delta^{13}C$ measurement for ODP Site 846 is located at 8.0°S, 85.84°W; 3.4 km and provides a value of −0.16‰ (Schmittner et al., 2017). The age model for ODP Site 846 is based on the original stratigraphy of (Mix et al., 1995) and indicates sedimentation rates of ~4 cm ka^{-1}.

3.3. Stable isotope data

Stable oxygen and carbon isotopes measurements were made at the Lamont-Doherty Earth Observatory (LDEO) on the epifaunal foraminifera *C. wuellerstorfi* and the infaunal foraminifera *Globobulimina spp*. (predominately *G. pacifica*). Specimens were prepared by first freeze drying the bulk sediment, washing it through a 63 μm sieve, and drying the greater than 63 μm fraction at 45 °C overnight. Between one and three specimens of each species were picked from the greater than 250 μm size fraction, weighed, and analyzed on a Thermo Delta V Plus with Kiel IV automated individual sample acid-reaction device. Values were calibrated to the VPDB isotope scale with NBS-19 and NBS-18. Reproducibility (one sigma) of the in-house standard over the interval of sample analysis was ±0.03‰ for $\delta^{13}C$ and ±0.06‰ for $\delta^{18}O$.

3.4. U-series data

Isotope measurements of U and Th were made using isotope dilution on an Element 2 ICP-MS at LDEO. For each measurement, ~100 mg of freeze-dried bulk sediment was spiked with ^{236}U and ^{229}Th prior to complete digestion using HNO_3, HF, and $HClO_4$. The dissolved U and Th fractions were isolated using Fe-hydroxide co-precipitation and anion-exchange column chemistry methods, following (Fleisher and Anderson, 2003). A blank and internal sediment standard were measured alongside each batch of measurements to determine data reproducibility. Blank concentrations were negligible for all isotopes and the long-term relative standard deviation for the standard is 3% for ^{238}U and 2% for ^{230}Th. For aU, the average propagated one sigma uncertainty (including counting statistics, mass bias corrections, counting gain corrections, and uncertainty in sample spike masses) is 0.04 ppm. Uncertainties for $^{230}Th_{xs,0}$ were propagated as above but also include propagated uncertainty due to the decay correction and thus uncertainties increase with age. The maximum one sigma uncertainty for $^{230}Th_{xs,0}$ is 0.17 dpm g^{-1} (less than 5% of the corresponding sample value).

3.5. Barium data

Sedimentary Ba and aluminum (Al) concentrations were measured at LDEO using an ICP-OES. For each sample ~50 mg of bulk sediment was digested using HNO_3, HF, and $HClO_4$. Samples were then dried down and taken up in a known volume of 0.5N HNO_3. Samples were run with five replicates of five known standards to constrain peak areas. The average one sigma standard deviation of these runs was 0.03 mg g^{-1} Ba or at maximum 0.8% of total Ba concentrations. Non-lithogenic Ba (Ba_{xs}) was quantified by using a $Ba/Al_{Terrigenous}$ ratio of 0.0075 (François et al., 1995) and fluxes were calculated by normalization to ^{230}Th (François et al., 2004). This approach assumes that Al is exclusively of detrital origin and that the lithogenic Ba/Al did not vary substantially in space or time. Corrections for the terrigenous fraction are less than 10% of the total measured Ba at ODP Site 1240.

4. New results

4.1. Stable isotopes

Benthic carbon and oxygen isotope values reconstructed from *C. wuellerstorfi* are quite similar between ODP Sites 1240 and 846 as might be expected given their close geographic proximity and similar water mass history (Fig. 4A, B, E and F). Oxygen isotope values show clear glacial-interglacial and precessional variability in keeping with the global (Lisiecki and Raymo, 2005) benthic oxygen isotope stack. The deglacial $\delta^{18}O$ values of *C. wuellerstorfi* at ODP Site 846 seem to suggest that there may be some issues with the core's age model during that interval. In the absence of additional constraints (*e.g.*: ^{14}C data) we have elected to maintain the original chronology as it does not substantially affect our interpretations.

In contrast with $\delta^{18}O$, the carbon isotope signatures of *Globobulimina spp.* are less consistent between the two sites, with generally higher amplitude variability at ODP Site 1240 and overall lower $\delta^{13}C$ at Site ODP Site 1240, especially prior to 50 ka (Fig. 4C and G, and Fig. 5). More broadly, the point-to-point variability in the $\delta^{13}C$ of *Globobulimina spp.* at both sites is much more pronounced

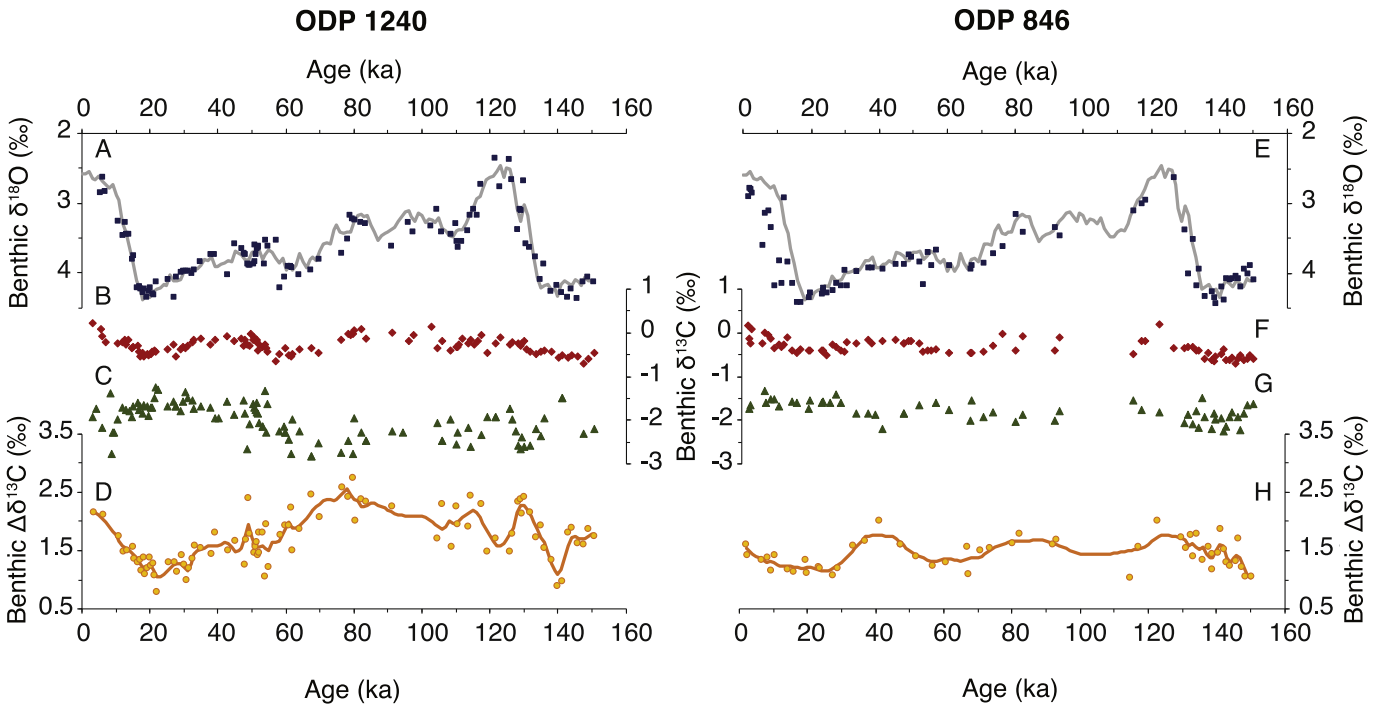

Fig. 4. ODP Sites 1240 and 846 Stable Isotope Summary. A and E) $\delta^{18}O$ of *C. wuellerstorfi* at ODP Sites 1240 and 846 respectively. The grey lines are the LR04 benthic stack (Lisiecki and Raymo, 2005). B and F) $\delta^{13}C$ of *C. wuellerstorfi*. C and G) $\delta^{13}C$ of *Globobulimina spp.* D and H) $\Delta\delta^{13}C$ derived from the epifaunal and infaunal foraminifera. The gold lines depict a three-point running mean of each data set.

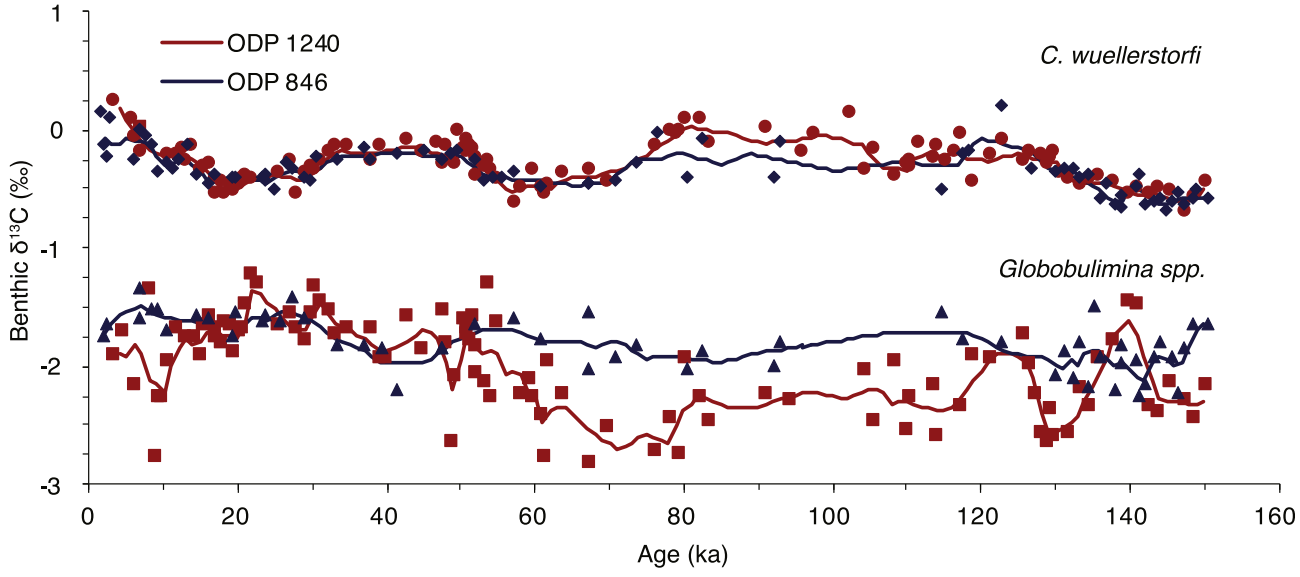

Fig. 5. ODP Sites 1240 and 846 Benthic Species Comparison. $\delta^{13}C$ of *C. wuellerstorfi* at ODP Site 1240 (red dots) and ODP Site 846 (blue diamonds). $\delta^{13}C$ of *Globobulimina spp.* at ODP Site 1240 (red squares) and ODP Site 846 (blue triangles). Solid lines depict the three-point running mean of each data set.

than in *C. wuellerstorfi*. Regressing the raw data against the three-point running mean of each data set (solid lines in Fig. 5) yields coefficients of determination (R^2 values) that illustrate this difference. For the *C. wuellerstorfi* carbon isotope records the R^2 values are 0.83 and 0.84 for ODP Sites 1240 and 846 respectively, while for *Globobulimina spp.* the values are 0.67 and 0.53. The carbon isotope differences between the two sites, primarily driven by differences in *Globobulimina spp.*, translate into pronounced differences in the $\Delta\delta^{13}C$ of the two sites, thus leading to substantially different BWO reconstructions (Fig. 6). Notably, the magnitude of $\Delta\delta^{13}C$ variability reconstructed at ODP Site 1240 is suggestive of oscillations of (on average) ~48 μmol kg^{-1} (from consecutive depth intervals with an average resolution of 2 ka), and ~37 μmol kg^{-1} at ODP Site 846 (with an average resolution of 3 ka). This magnitude of variability, on oceanographically-short timescales, is too large to be explained by basin-wide changes in oxygen availability and is thus suggestive of other influences on the $\delta^{13}C$ of *Globobulimina spp.*

Beginning with the oldest parts of the $\Delta\delta^{13}C$ records at ~150 ka during Marine Isotope Stage (MIS) 6 (Fig. 6), values suggest generally increasing BWO concentrations during the late glacial, although there is quite a bit of scatter in the records. Increasing BWO concentrations continue through Termination II in both

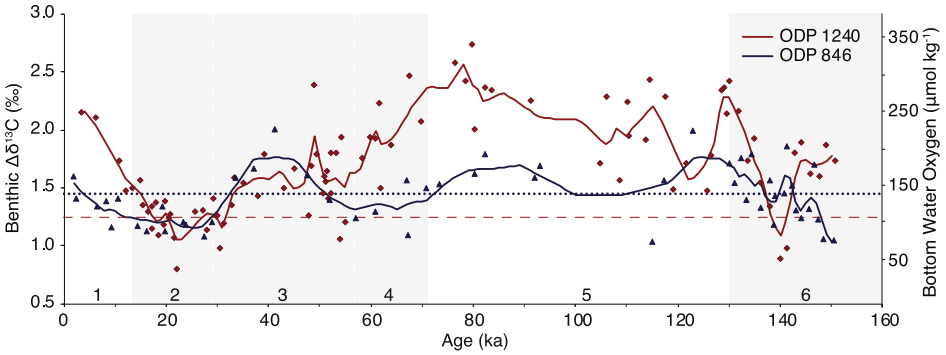

Fig. 6. ODP Sites 1240 and 846 $\Delta\delta^{13}C$ Comparison. $\Delta\delta^{13}C$ and corresponding BWO concentration using the calibration of (Hoogakker et al., 2015). Red line and diamonds for ODP Site 1240 and blue line and triangles for ODP Site 846. Both lines depict the three-point running mean of each data set. Horizontal lines show the modern BWO for ODP Site 1240 (dashed red line) and ODP Site 846 (dotted blue line). Marine Isotope Stages (MIS) are denoted at the bottom of the figure with the grey background indicating glacial stages.

records, however the respective magnitudes of change are different with ODP Site 1240 reaching peak MIS 5e oxygen concentrations of ~240 μmol kg^{-1} by 130 ka (~130 μmol kg^{-1} or ~120% higher than at present) and ODP Site 846 reaching ~ 170 μmol kg^{-1} (~30 μmol kg^{-1} or ~30% higher than at present). Between 130 and 120 ka the records both show a decrease in BWO (although of different magnitudes), and after 120 ka the records are characterized by a general increase in values to higher BWO concentrations around 80 ka. At ODP Site 1240 this maximum BWO value (from the three-point smooth) is ~280 μmol kg^{-1}, 2.6 times higher than modern oxygen concentrations at the site. After 80 ka, perhaps coincident with the last glacial inception, both records show a decline in BWO values, although they disagree about the precise onset and the magnitude of decline, as well as the magnitude of millennial-scale variability. By 20 ka the records have come close to converging on an LGM BWO concentration somewhere in the range of 80–95 μmol kg^{-1} with ODP Site 846 recording a higher value. During the deglaciation, both records reconstruct a rise in BWO concentrations, although the increase is much larger (and therefore more rapid) at OPD 1240. Core-top BWO reconstructed for ODP Site 1240 is 226 μmol kg^{-1}, and 154 μmol kg^{-1} at ODP Site 846. These core top oxygen reconstructions are higher than at present by 110% (119 μmol kg^{-1}) and 15% (20 μmol kg^{-1}) for ODP Sites 1240 and 846 respectively.

4.2. U series data

The trends in BWO reconstructed using aU broadly parallel those reconstructed based on the $\Delta\delta^{13}C$ proxy at ODP Site 1240 (Fig. 7). Both proxies suggest low BWO during MIS 6 with a steep

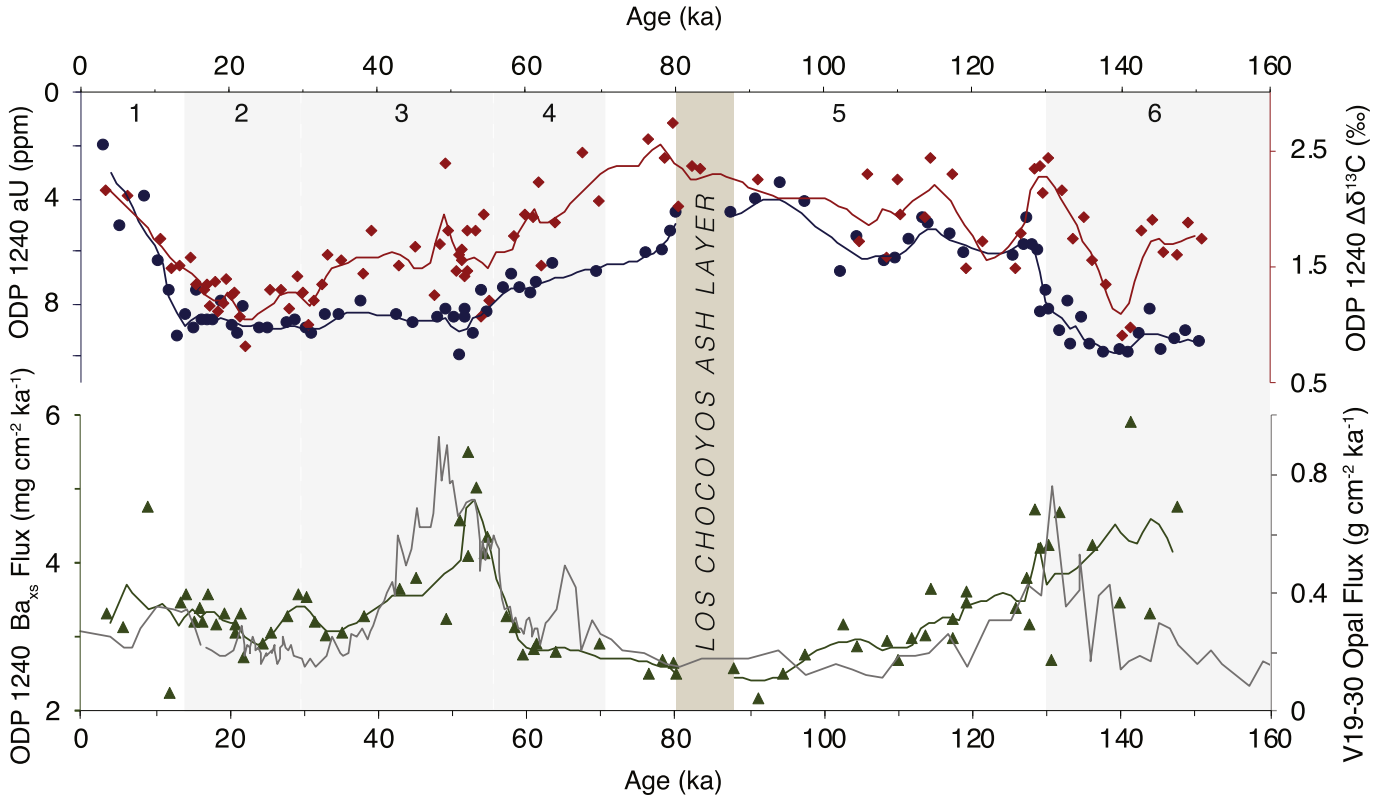

Fig. 7. Comparison of $\Delta\delta^{13}C$, aU and Productivity. New records from ODP Site 1240 along with the opal flux record from nearby site V19-30 (Hayes et al., 2011). A) $\Delta\delta^{13}C$ (red diamonds and line, y axis at right) and aU (blue circles and line, y axis at left). B) Ba_{xs} flux (green triangles and line) and opal flux (grey line). Lines depict the three-point running mean of data sets except for opal where it depicts the raw data. The brown bar identifies the core interval associated with the deposition of the Los Chocoyos ash layer. MIS as in Fig. 6.

deglacial rise in oxygen concentrations persisting, with some variability, until MIS 5c at approximately 95 ka. Subsequent to MIS 5c aU concentrations increased until ~50 ka. The exact timing of the aU increase and BWO decrease relative to MIS 5c is difficult to assess for reasons discussed below. The aU-based reconstruction suggests that O_2 concentrations remained low from ~50 ka to 15 ka, at which point they rose rapidly through the deglaciation until they reached the well-oxygenated Holocene conditions that characterize the site today. Notably, the timing of the MIS 5c decrease in BWO and the deglacial rise does not appear to be consistent when considering downcore aU and $\Delta\delta^{13}C$ records in tandem (Fig. 7A). The $\Delta\delta^{13}C$ record appears to suggest that BWO concentrations remained at interglacial levels until around 78 ka (closer to the end of MIS 5a). The precise magnitude of the temporal offset between these two records is difficult to determine due to the presence of the Los Chocoyos ash layer (Drexler et al., 1980) and its influence on the aU record through probable changes in the $^{238}U/^{232}Th$ ratio during the ash deposition (Supplementary Note 2). The offset between the onset of oxygen decrease recorded by aU and $\Delta\delta^{13}C$ could be as large as 17 ka or as small as 2 ka (Supplementary Fig. 1). The aU and $\Delta\delta^{13}C$ records also provide different timelines for the deglacial rise in oxygen with the rise reconstructed from $\Delta\delta^{13}C$ occurring ~5 ka earlier than suggested by the aU record. We investigate these discrepancies in the context of productivity and the other various controls on the two proxies in Section 5.1.

4.3. Barium flux data

Because of the significance of organic carbon flux in controlling sedimentary redox state and aU precipitation, Ba_{xs} fluxes were measured in tandem on ODP Site 1240 sediments (Fig. 7B). The new record confirms the general productivity patterns previously identified at a nearby EEP site using opal fluxes (Hayes et al., 2011), with higher productivity during deglacial transitions and a strong pulse of productivity near 50 ka. Both records are therefore of value in characterizing the regional productivity of the EEP.

5. Discussion

5.1. Core intracomparison

ODP Site 1240 is the only site in the equatorial Pacific Ocean where all three proxy approaches detailed in section 2 have been applied, and where a co-located record of export productivity is present (Fig. 8). Specifically, this study presents new aU, $\Delta\delta^{13}C$, and Ba_{xs} flux data spanning the past 150 ka. Alkenone biomarker concentrations are from Calvo et al. (2011) and we also include ^{14}C-based ventilation ages published by de la Fuente et al. (2015)

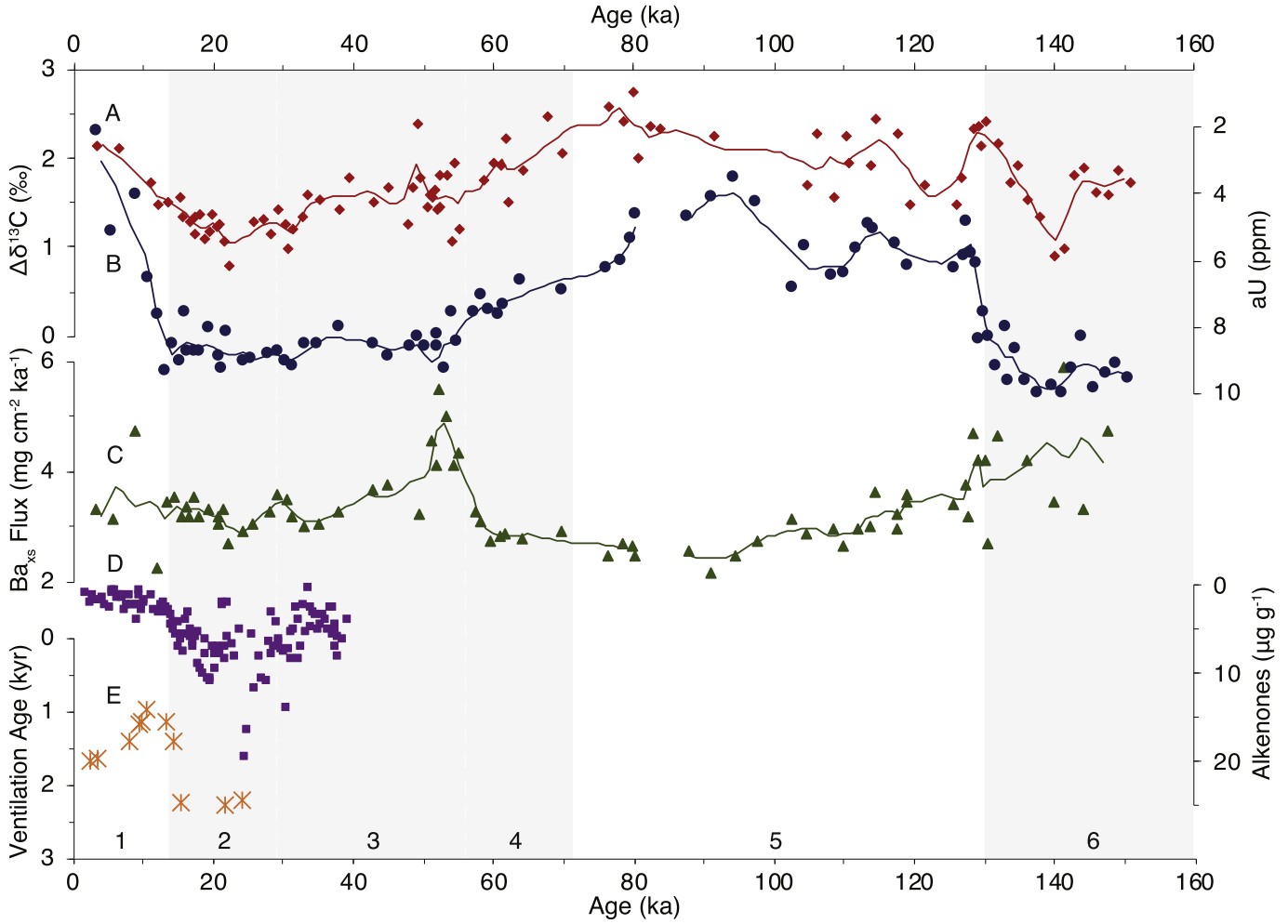

Fig. 8. Intra-Comparison of ODP Site 1240 Records. New records of A) $\Delta\delta^{13}C$ (red diamonds and line), B) aU (blue circles and line), and C) Ba_{xs} flux (green triangles and line). D) Alkenone concentrations from (Calvo et al., 2011) (purple squares). E) ^{14}C-derived water mass ventilation ages from (de la Fuente et al., 2015) (gold asterisks). All records have been placed on the age model of (Rippert et al., 2017). Lines depict three-point running means of data sets. MIS as in Fig. 6.

(Fig. 8). Intra-core comparison of these proxies allows us to investigate the differences in event onset and rates of change using co-registered data points. These intra-core comparisons are critical for understanding the biases inherent to each proxy, differences which may be important for our interpretation of these proxies on larger geographic and/or temporal scales.

The proxy records from ODP Site 1240, displayed in Fig. 8, consistently indicate low BWO concentrations during glacial periods with deglaciations reflecting transitions to better ventilated deep waters concurrently with the decrease in ^{14}C ventilation age (Fig. 8E). To investigate this shared variability in detail we begin by examining the oldest portion of the records, where both aU and $\Delta\delta^{13}C$ suggest a similar transition towards better oxygenated bottom waters at the penultimate deglaciation (138-128 ka). The records show some concordant variability within MIS 5 which does not appear to be attributable to the influence of organic carbon flux (Fig. 8C). Around the time of the MIS 5/4 transition (~71 ka) both aU and $\Delta\delta^{13}C$ suggest decreasing BWO and increased respired carbon storage. Both records indicate decreasing BWO until ~50 ka when aU formation appears to reach a steady-state, whereas $\Delta\delta^{13}C$ values continue to decline through to the last glacial maximum around 20 ka. The agreement between the ODP Site 1240 records of aU and $\Delta\delta^{13}C$, and their general lack of correlation with Ba_{xs} flux, lends support to the interpretation that the two records primarily reflect BWO rather than C_{org} supply.

Although the proxy reconstructions agree about the large-scale sense of G-IG changes in BWO, examination of the sense of smaller scale features, especially in light of their relationship with productivity (Ba_{xs} flux – Fig. 8C), and the precise timing and rate of proxy change, is useful in assessing the different controls on proxy production and preservation. We begin our examination by focusing on the interval between ~55 and 45 ka associated with a large productivity peak - as seen in both the Ba_{xs} flux from ODP Site 1240, and a nearby record of opal flux (Hayes et al., 2011) (Fig. 7). Associated with this productivity increase we report an increase in the sedimentary concentration of aU (note the reversed y axis), which could be interpreted as either a decrease in BWO, or a change in porewater redox state in response to increased organic carbon rain and respiration (Fig. 2B and C). Given the timescale of the excursion (short) and its association with the productivity peak we suggest the latter interpretation is more likely.

Between ~55 and 45 ka, during the interval with the productivity pulse, we observe positive excursions in the $\Delta\delta^{13}C$. The proxy interpretation proposed by Hoogakker et al. (2015) would translate this change as a basin-wide increase in bottom water ventilation. Note that this interpretation is in diametric opposition to the interpretation derived from the aU data, and apparently inconsistent with our preferred interpretation of decreased porewater oxygen availability due to enhanced C_{org} respiration. Closer investigation of the cause of the $\Delta\delta^{13}C$ change over this interval indicates that significant variability in the $\delta^{13}C$ of *Globobulimina spp.* may be driving the sedimentary $\delta^{13}C$ gradient (Fig. 4C). One possible source of high-frequency variability in *Globobulimina spp.* is that the foraminifera are recording variations in $\delta^{13}C$ that are a function of an additional influence other than oxygen-dependent respiration. Based on recent research on *Globobulimina spp.*, we highlight two mechanisms which may contribute isotopically light carbon to foraminifera tests, independent of variations in porewater oxygen concentrations.

A number of recent studies have shown that some benthic foraminifera can use an electron acceptor other than oxygen as an energy source (Glock et al., 2013; Høgslund et al., 2008; Risgaard-Petersen et al., 2006). Included in the genera of benthic foraminifera that have been shown to concentrate nitrate (likely indicating the ability to denitrify) are four species of *Globobulimina*, including *G. affinis* (Nomaki et al., 2015; Piña-Ochoa et al., 2010a), *G. pacifica* (Glock et al., 2013), *G. turgida* (Piña-Ochoa et al., 2010b) and *G. pseudospinescens* (Risgaard-Petersen et al., 2006). Indeed in *G. turgida*, aerobic and anaerobic survival and metabolic rates were observed to be the same (Piña-Ochoa et al., 2010b), indicating that *G. turgida* has no preference for oxygen over nitrate as an electron acceptor.

These new data provide robust evidence that *Globobulimina spp.* are at minimum facultative anaerobes and can likely be classified as functional anaerobes. A depth habitat for *Globobulimina spp.* below the sedimentary oxic-anoxic boundary presents two challenges to the $\Delta\delta^{13}C$ proxy as currently calibrated. First, the denitrification of *Globobulimina spp.* will actively decrease porewater $\delta^{13}C$ profiles below the depth where oxygen approaches zero, thus 'contaminating' foraminifera tests with light carbon unrelated to the oxic respiration of organic matter (and unrelated to BWO concentrations). Offsets might be expected to be small where the carbon isotope gradient has a shallow slope (low productivity environments), but could be significant at higher productivity sites (McCorkle et al., 1985), especially where nitrate is abundant as it is in the deep Pacific Ocean. Second, since the depth habitat of *Globobulimina spp.* is not limited by oxygen, the foraminifera may live deeper in the sediment than previously thought and, therefore, may be more susceptible to the upward diffusion of light carbon from sulfate reduction (McCorkle and Emerson, 1988). Both of these effects would be expected to be more significant at low BWO concentrations where more organic carbon escapes oxic respiration and can support denitrification and sulfate reduction.

In sum, we argue that the $\Delta\delta^{13}C$ proxy is subject to variable but potentially significant contributions of isotopically light carbon from anaerobic processes - both denitrification and sulfate reduction (McCorkle and Emerson, 1988) - which can 'alter' reconstructions of O_2 based on the $\Delta\delta^{13}C$ approach. The more anaerobic respiration that occurs, perhaps a function of organic carbon or nitrate availability, the greater the signal distortion. Specifically, during intervals characterized by constant BWO but increased organic carbon flux, we would predict that the $\delta^{13}C$ of *Globobulimina spp.* would decrease, causing an increase in the $\Delta\delta^{13}C$ and leading to an incorrect inference of higher BWO. Indeed, some authors have previously suggested that benthic $\Delta\delta^{13}C$ gradients might be used to quantify organic carbon fluxes (Mackensen and Licari, 2003; Schmiedel and Mackensen, 2006), and several genera of benthic foraminifera were recently used for just such a calibration (Theodor et al., 2016). Our conclusions about the potential for isotopically light carbon to 'contaminate' the $\Delta\delta^{13}C$ proxy holds true for reconstructions using *Globobulimina spp.*, and also for any other infaunal species living in environments in which anaerobic respiration is releasing isotopically light carbon. Because aerobic respiration and denitrification can proceed concurrently in the sediment, our findings are important to consider even at sites where BWO is high.

Although the $\Delta\delta^{13}C$ proxy for BWO appears likely to be influenced by variables other than ventilation-related oxygen availability, we argue that it is still a useful proxy, especially in tandem with records like aU, which may experience proxy 'distortions' of an opposite sense (Gottschalk et al., 2016). Returning to the example of ODP Site 1240 between 55 and 45 ka, we can see that the antiphase response of $\Delta\delta^{13}C$ and aU could logically be attributed to a greater rate of supply of organic matter to the site – that is, the additional organic matter fuels increased aU precipitation, interpreted as lower BWO, while concurrently supporting a greater anaerobic contribution of light ^{13}C to infaunal species, leading to the opposite interpretation of greater BWO. We can thus discard this local variability when examining ventilation-related changes in BWO on a regional scale. In contrast, when variability in aU and $\Delta\delta^{13}C$ is

concordant, as it is between 140 and 110 ka, we have greater confidence in our interpretation of the proxies as indicative of changes in basin-wide BWO and respired carbon contents.

5.2. Proxy intercomparison

5.2.1. aU

Records of aU provide the most abundant equatorial Pacific BWO reconstructions. Twenty-two records of aU have been published, in part as a byproduct of extensive U-series measurements generated in the pursuit of flux-normalized export productivity and dust reconstructions. Previous work has presented a subset of these records (Bradtmiller et al., 2010), and here we expand on that treatment, including cores at both the highest (16.4 cm ka^{-1}) and lowest (1.2 cm ka^{-1}) sedimentation rate sites available, and at the deepest (4.4 km) and shallowest (1.9 km) water depths. As a consequence of the breadth of our survey, we include records that have accumulated in a wide range of sedimentary environments and have experienced different degrees of post-depositional alteration. A compilation of the timeseries records can be seen in Fig. 9 A.

The equatorial Pacific records of aU display a wide range both in the quantity of aU present in the sediments, and in the timing of the peak aU accumulation. The first observation reinforces the point that aU cannot be treated as a quantitative indicator of BWO conditions. For example, the ML1208 cores (37BB, 31BB and 17 PC) are tightly clustered in space, yet ML1208-37BB contains no aU, while ML1208-17 PC has concentrations approaching 3 ppm. We suggest that these differences are to first order a function of the different organic carbon fluxes at the sites (Jacobel et al., 2017). With the influence of organic carbon flux in mind it is unsurprising that the core with the highest LGM sedimentation rate (MV1014-17JC, 16.4 cm ka^{-1}) also has the highest aU content. Assuming that the sedimentation rate approximately scales with the amount of organic carbon delivery at a site, higher aU accumulation would be expected in a site with greater sedimentation. The patterns observed in these equatorial Pacific cores thus provide ample support for the idea that aU records should be interpreted only in the context of a site-specific record of organic productivity, preferably one that is flux normalized.

The four aU records discussed thus far illustrate a relatively predictable relationship between aU and organic carbon accumulation rates. Unfortunately, this relationship is not always so straightforward. Fig. 9B, illustrates that aU content does not scale linearly with sedimentation rate. Instead, some cores with lower sedimentation rates have high LGM aU (*e.g.*: RC13-114 at 2.8 cm

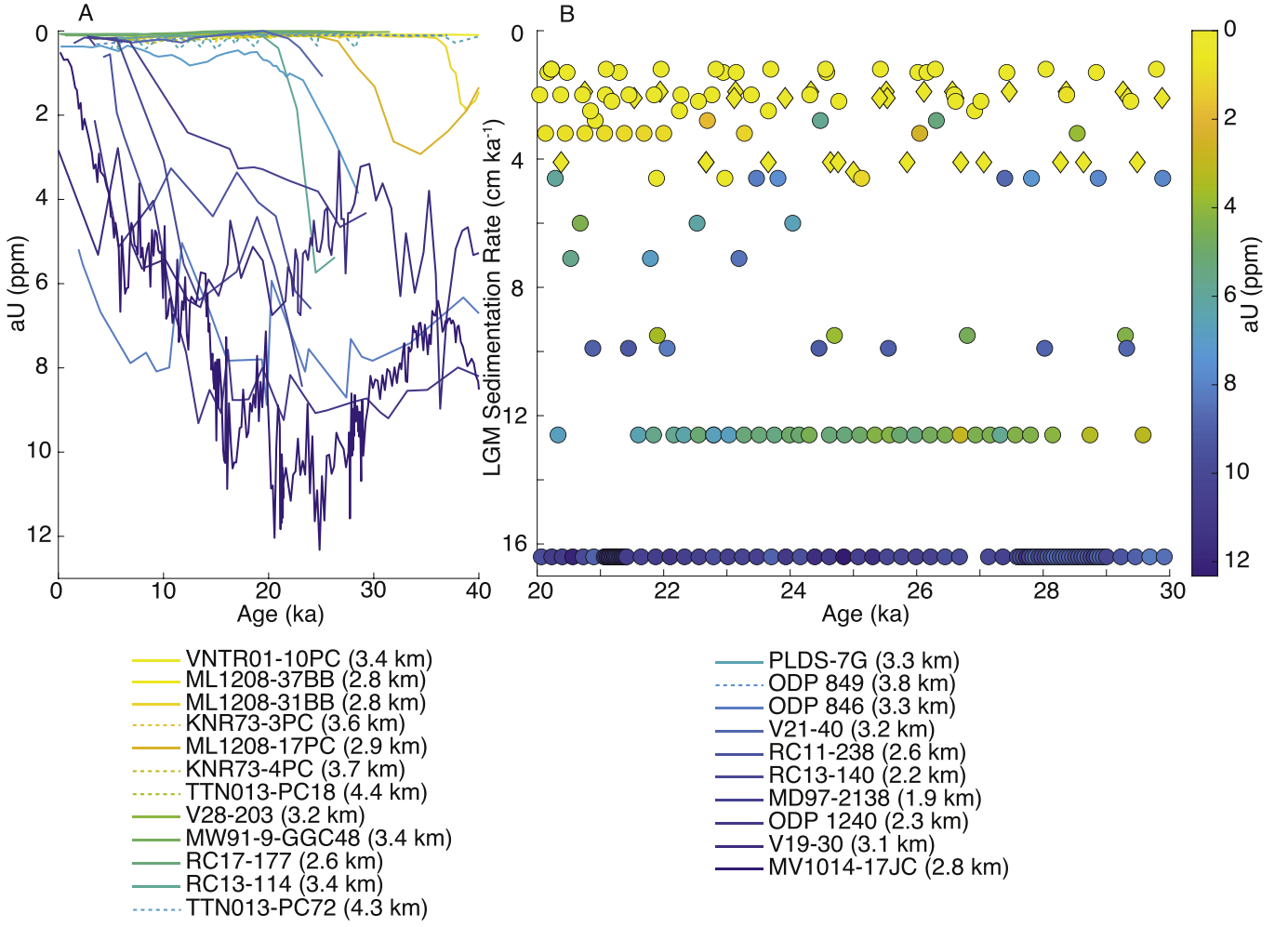

Fig. 9. Equatorial Pacific Records of aU. A) Twenty-two aU timeseries arranged and color coded by sedimentation rate over the time interval from 20 to 30 ka (blue = high, yellow = low). Cores with sedimentation rates below 3 cm ka^{-1} are listed on the left, above 3 cm ka^{-1} on the right. Solid lines depict cores above 3.5 km, dotted lines depict cores below 3.5 km. B) Core aU contents from 20 to 30 ka in colors (blue = high, yellow = low) with the cores spread out along the y-axis according to sedimentation rate. Dots depict cores above 3.5 km, diamonds depict cores below 3.5 km.

ka^{-1}) and others with high sedimentation rates appear to have little or no LGM aU accumulation (*e.g.*: ODP 849 at 4.4 cm ka^{-1}). Departures from a simple trend may be due to local variations in sediment transport (*e.g.*: Kienast et al., 2007), export productivity (*e.g.*: Costa et al., 2017), or post-depositional remobilization of aU (*e.g.*: Jacobel et al., 2017). Once again, these variations highlight the need for flux-normalized records of organic matter supply to the sediments.

One of the reasons for divergent aU contents in cores with similar sedimentation rates may relate to post-depositional burndown (*i.e.* oxygenation and re-mobilization) of aU. Burndown may also explain heterogeneity in the apparent timing of deglacial oxygenation. In several cores with sedimentation rates lower than ~3 cm ka^{-1}, aU concentrations appear to have begun to decline or already reached values near-zero by 25 ka (Fig. 9A). This is despite a lack of evidence for any deglacial change in ventilation as early as 25 ka. We propose that the reason for these apparent declines is post-depositional reoxygenation of sediments and release of aU to bottom waters, combined in some cases the re-precipitation of mobilized U downcore. Indeed, the release of aU to bottom waters may well explain why some sites with low accumulation rates do not appear to have any aU preserved. Tandem measurements of proxies with opposing redox behavior (*e.g.*: aU and Mn) may help clarify some of the apparent contradictions in these records and should be an area of future study. We suggest that burndown makes assigning the timing of deglacial bottom water oxygenation, and glacial inception oxygen limitation difficult, if not impossible, in slowly accumulating marine sediments.

Previous work has interpreted the absence of aU preservation in cores below 3.5 km as indicative of the persistence of better ventilated southern-sourced waters (LCDW) than the overlying return flow at the LGM (Jacobel et al., 2017; Thiagarajan and J. F. McManus, 2019). Because the preservation of aU in slowly accumulating sediments (most sites below 3.5 km) is not guaranteed, we recommend a more conservative approach to interpreting these records. We contend that an absence of aU evidence for low BWO is not evidence that such conditions were absent. Other redox-sensitive proxies, such as Mn, may help to elucidate this question at sites where glacial aU is not observed.

5.2.2. $\Delta\delta^{13}C$

Due to the relatively recent development of a calibration for the $\Delta\delta^{13}C$ proxy, it has not yet been applied extensively in the Pacific Ocean. The existing records are located in and around the Panama Basin in the eastern equatorial Pacific Ocean. The close proximity of these three previous records (Hoogakker et al., 2018; Umling and Thunell, 2018) and our two new records from ODP Sites 1240 and 846 (Fig. 10), thus provide an interesting test case for intercomparison. All reconstructions have used the epifaunal *C. wuellerstorfi*, infaunal *Globobulimina* species and applied the calibration of (Hoogakker et al., 2015). Despite these common conventions, the five datasets record quite different $\Delta\delta^{13}C$ values from one another and also suggest significantly different Holocene $\Delta\delta^{13}C$/BWO values from the conditions that prevail at these sites today. Here we investigate these discrepancies and their possible cause(s).

As previously discussed in Section 4.1 there are considerable differences between the $\Delta\delta^{13}C$ of the two longest records, ODP Sites 1240 and 846. At times the sites disagree about the magnitude of BWO concentrations by more than 125 μmol kg^{-1} with ODP Site 1240 showing considerably higher values throughout most of the record. This is unexpected given the shallower depth of ODP Site 1240, located more completely within the return flow of low-oxygen Pacific Deep Water. While the magnitude of reconstruction spread is considerably smaller at the LGM, even with more records present, it still amounts to ~56 μmol kg^{-1} meaning that the most oxygenated reconstruction (ODP Site 1240, at 2.3 km) suggests BWO concentrations were twice as high as the least oxygenated reconstruction (TR163-25, at 2.7 km). Interpretation of either of these individual records as representative of the Pacific would thus yield vastly different estimates of respired carbon storage at the LGM.

Examining the latest-Holocene data points for each of the records and modern BWO concentrations at the five sites we see further evidence of data-data and data-observation mismatches. Although TR163-25 and ODP Site 846 agree about the early Holocene BWO concentration within uncertainty (±17 μmol kg^{-1}), the total range of reconstructed BWO concentrations between the sites is almost 160 μmol kg^{-1} (compare ranges among lines at 4 ka in Fig. 10). Even more concerning is the lack of correspondence between the reconstructions and measured BWO concentrations at

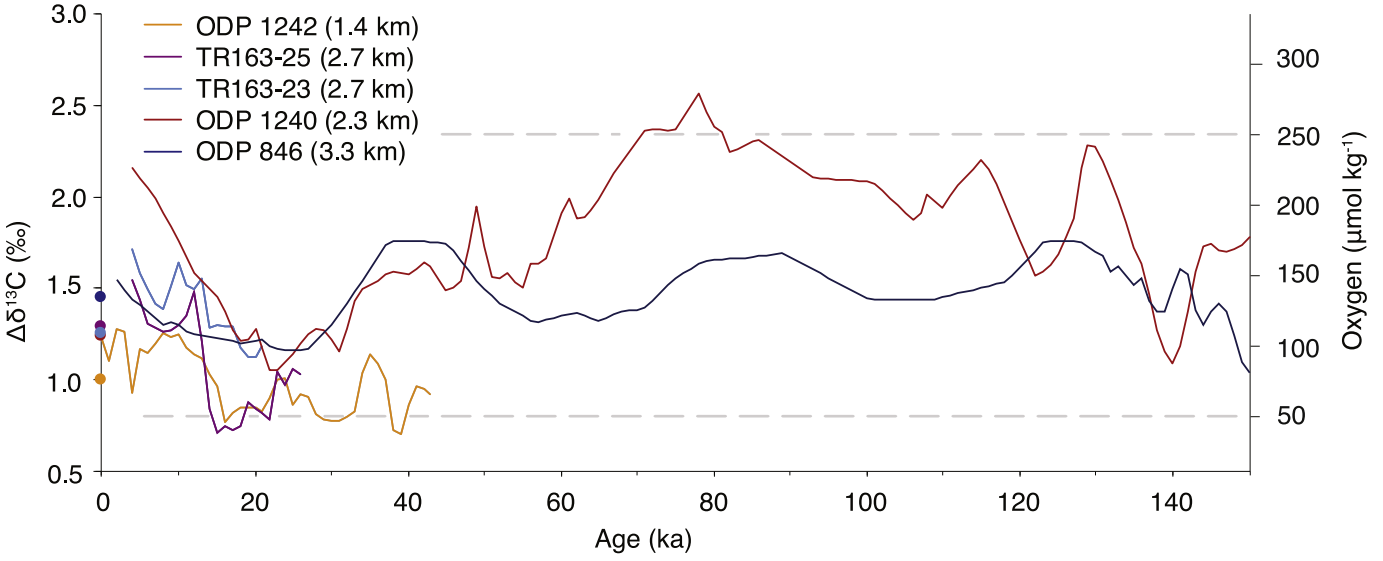

Fig. 10. Equatorial Pacific Records of $\Delta\delta^{13}C$. New data from ODP Site 1240 (red line) and ODP Site 846 (navy blue line) with previously published records from ODP Site 1242 (gold line) and TR163-25 (purple line) and TR163-23 (light blue line). Grey dashed lines denote the lower and upper bounds of the proxy calibration from (Hoogakker et al., 2015). The dots at left correspond to the modern-day BWO concentrations (converted to $\Delta\delta^{13}C$) at each of the five sites (dot colors correspond to site/line colors).

the five sites as illustrated by the mismatch between proxy data reconstructions (lines) and modern observations (dots) in Fig. 10. Given that we have no reason to suspect that early-to-mid Holocene BWO concentrations were higher than today, the observation of values ranging from 20 to 120 μmol kg^{-1} higher than modern observations (ODP Site 846 is the closest to modern observations, ODP Site 1240 is the furthest) gives us reason to question all five reconstructions. Taking the LGM BWO reconstructions of these cores *at face value* and calculating the magnitude of LGM-Holocene carbon release using reconstructed Holocene values yields estimates of respired carbon storage that differ from what would be calculated using measured modern values of BWO by up to 472 GtC (i.e., using ODP Site 1240 reconstructed core top BWO vs. measured modern BWO) (Supplementary Note 3). Not only is the reconstructed magnitude of carbon release dramatically different from what would be calculated using modern measurements, the range of estimates of LGM-Holocene changes in C storage varies by ~440 GtC among the different records (maximum at ODP Site 1240, minimum at ODP Site 1242). These uncertainties are arguably too large to yield meaningful paleoclimate reconstructions.

It is significant that all of the late-Holocene reconstructions yield estimates of BWO that are higher than modern values. This finding is consistent with our hypothesis that the incorporation of anaerobically produced low $\delta^{13}C$ into Globobulimina spp. drives up estimates of O_2 relative to the prediction of the theoretical model that is premised upon strictly oxic respiration. Indeed, there appears to be a linear relationship between bulk sedimentation rate and the magnitude of offset between the observed and reconstructed BWO at four of the sites (Supplementary Note 4 and Supplementary Fig. 2). Assuming that the incorporation of 'extra' low $\delta^{13}C$ produced by anaerobic respiration is the dominant process leading to divergent $\Delta\delta^{13}C$ reconstructions (either via denitrification or sulfate reduction), the implication is that $\Delta\delta^{13}C$-based BWO reconstructions will be consistently, though variably, biased towards high BWO estimates. This renders LGM reconstructions absolute maximum estimates, placing the true BWO concentrations at or below reconstructed values. A critical corollary to this observation is that $\Delta\delta^{13}C$-derived estimates of deep ocean respired carbon storage reflect *minimum* estimates, and thus the ocean may have been an even larger sink for CO_2 than published reconstructions suggest. We therefore recommend that 1) the $\Delta\delta^{13}C$ proxy be applied as a semi-quantitative indicator of *maximum* BWO, 2) sites where the core top BWO reconstruction is in excess of modern site-specific values be treated with particular caution, and 3) abrupt variations in $\Delta\delta^{13}C$ be interpreted with significant skepticism and only in tandem with reliable paleoproductivity indicators.

5.2.3. Biomarkers

A recent compilation of Pacific biomarker data (Anderson et al., 2019) combined the observation of lower fluxes of inorganic (opal, $^{231}Pa/^{230}Th$, and Ba_{xs}) productivity indicators (Costa et al., 2017, 2016; Winckler et al., 2016) during the last glacial period with the observation of higher sedimentary biomarker concentrations to argue that BWO concentrations were lower during the last glacial period relative to the Holocene. This conclusion, detailed in Anderson et al. (2019), is based on a wealth of studies in different environments (*e.g.*: Cowie et al., 2014; Keil and Cowie, 1999; Koho et al., 2013; Lengger et al., 2014; Rodrigo-Gámiz et al., 2016; Sinninghe Damsté et al., 2002) suggesting that the sensitivity of biomarker preservation to variables such as sediment accumulation and grain size is secondary compared to the sensitivity to oxygen exposure time. Here, we expand on the number of datasets included in that compilation (Fig. 11), but arrive at the same conclusions (see below).

An important contribution of these proxy data sets is that they

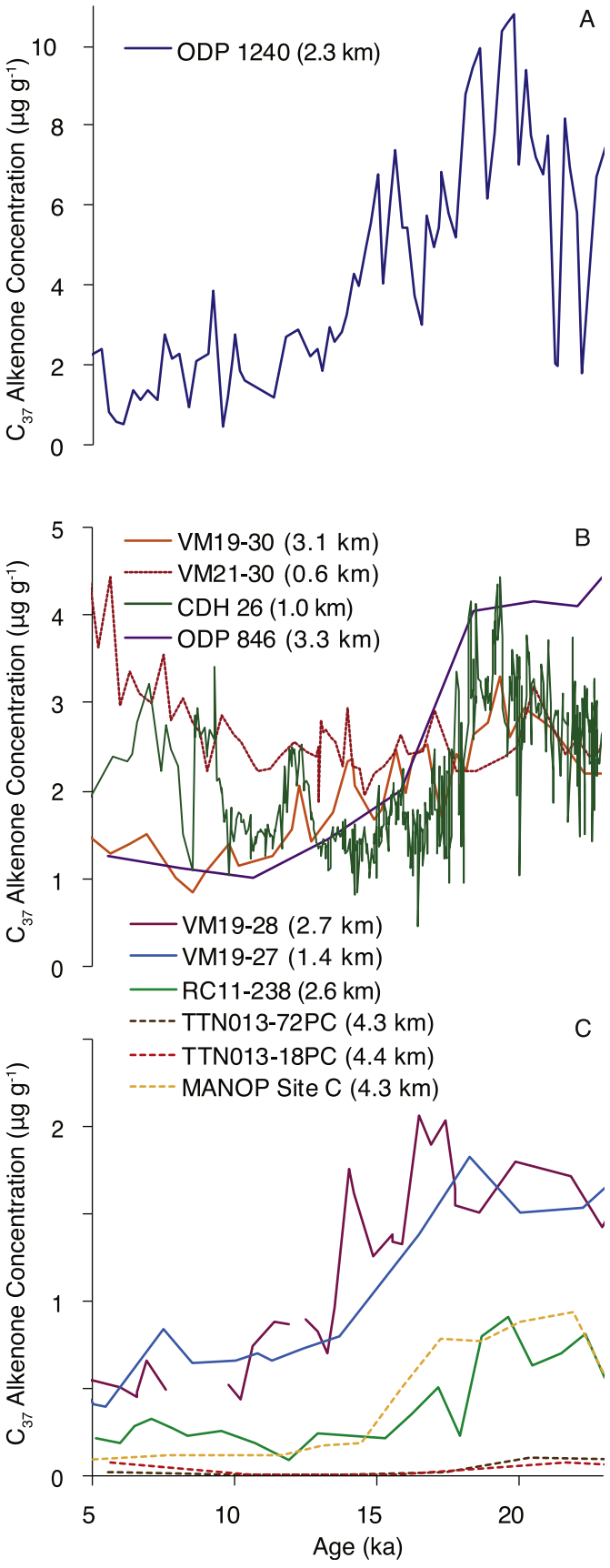

Fig. 11. Equatorial Pacific Records of Preserved Biomarkers. C_{37} Alkenone concentrations for equatorial Pacific cores. Note that panels A, B and C have different y-axis scaling for ease of visualization. Dashed lines indicate cores below 3.5 km, solid lines indicate cores above 3.5 km, dotted line indicates core at 0.6 km.

answer the question of *where* in the Pacific oxygen was reduced during the LGM, and thus where the bulk of respired carbon was stored. In striking contrast with the ambiguity of the aU records, the biomarker preservation records conclusively demonstrate that LGM oxygen availability was lower in both NPDW and LCDW. This is best illustrated in panel C of Fig. 11, which documents deglacial changes in biomarker preservation in all three records below 3.5 km (dotted lines). Following Anderson et al. (2019) we present these records in concentrations space rather than flux as ^{230}Th data are not available for all sites. Where flux data are available (including sites in the central equatorial Pacific, eastern equatorial Pacific, and easternmost equatorial Pacific) the alkenone concentration trends match flux-normalized trends, indicating that focusing cannot account for these results (see Fig. 5 in Anderson et al., 2019).

While our compilation adds additional spatial constraints to the LGM oxygen reconstruction, our conclusions are entirely consistent with the results presented by Anderson et al. (2019). Based on the preservation patterns observed, whereby alkenone concentrations in ice-age sediments at all sites studied are consistently much greater than during the Holocene despite evidence for lower (or unchanged) rates of organic matter supply, we suggest that the entire Pacific Ocean below 0.6 km was more poorly oxygenated during the LGM relative to present. Using our spatial coverage of the equatorial Pacific, we propose that water masses at the modern day depths of LCDW, NPDW, and AAIW were all more poorly oxygenated during the LGM than at present.

Evidence of oxygen-driven changes to biomarker preservation in the deepest Pacific where sites are presently bathed by LCDW suggests that 1) aU deposited under lower BWO conditions of the LGM has been remobilized subsequently following the deglacial rise in BWO or 2) BWO concentrations were sufficiently low to change biomarker preservation but not sufficiently low for the precipitation of aU. Although biomarker preservation appears to be a more appropriate BWO proxy for the deepest Pacific sites, we suggest that the proxy is still limited in its ability to resolve the timing of deglacial ventilation (which aU is also unable to provide). Because oxygen can diffuse into the sediments, previously buried organic biomarkers are not necessarily immune to oxygen exposure that might reduce their preservation (*e.g.*: Colley et al., 1989; Colley and Thomson, 1985; De Lange, 1998, 1986; Prahl et al., 1989a). This 'burndown', in addition to local variations in deglacial productivity, may help to explain the discordant timing of the biomarker records. These effects may be less important in high accumulation rate sites, but in the absence of quantitative information about the length scales of organic biomarker burndown we are hesitant to draw further conclusions. Further work comparing high-resolution records of redox-sensitive trace elements and biomarkers may help to resolve this question.

5.3. Synthesis

Oxygen concentrations in the deep equatorial Pacific reflect the integrated history of organic carbon remineralization from the time of last air-sea ventilation to the site at which they are measured. Reconstructed oxygen concentrations may therefore reflect changes occurring at any point along the transit pathway, from changes in the rate of organic carbon remineralization at the source, to changes in the flux of organic carbon to the site where measurements are made. Although this work has focused on the equatorial Pacific, the most significant changes to deep Pacific water masses likely originate in the Southern Ocean where the ocean's soft tissue biological pump has the greatest potential for increases in efficiency (Sigman and Boyle, 2000; Sigman et al., 2010). A suite of glacial changes including increased stratification, decreased upwelling, greater dust fertilization, and greater CO_2 solubility were critical for enhancing glacial carbon storage (*e.g.*: Bereiter et al., 2018; Francois et al., 1997; Jaccard et al., 2013; Martínez-García et al., 2014; Sigman et al., 2004; Studer et al., 2015). At ODP Site 1240 the approximate onset of increasing aU accumulation at ~90 ka (Fig. 8) ties in well with decreases in pCO_2 as reconstructed from Antarctic ice cores (Lüthi et al., 2008). The timing of the shift in aU precipitation, separate from any local changes in organic carbon flux, suggests that this change to less oxygenated conditions reflected a Pacific-wide increase in respired carbon storage in association with the changes to ocean physics and biological productivity originating in the Southern Ocean. The $\Delta\delta^{13}C$ data from ODP Site 1240 show a slightly later onset of this change but we attribute the observed temporal offset to the paucity of data between 80 and 90 ka rather than a significant disagreement between the BWO proxies. Both the aU and $\Delta\delta^{13}C$ records from ODP Site 1240 indicate that there was a long-term drawdown of oxygen levels in the deep Pacific from 90 to 20 ka, independent of local changes in productivity. Indeed, there is no evidence that dust increased productivity in the equatorial Pacific during the last glacial period, neither in the western Pacific (Winckler et al., 2016), nor in the central Pacific (Costa et al., 2016; Winckler et al., 2016), nor in the eastern Pacific (Thiagarajan and J. F. McManus, 2019; Winckler et al., 2016), and not in the easternmost Pacific (Jacobel et al., 2019). Although export production and dust delivery in the equatorial Pacific can change with climate, these changes have not been observed to correlate with changes in the net efficiency of the biological pump (Robinson et al., 2009). During the last glacial period there is strong evidence for enhanced nutrient utilization in waters upstream from the equatorial Pacific (Martínez-García et al., 2014), indicating that waters reaching the equatorial Pacific were in fact relatively nutrient poor and did not support enhanced productivity relative to present (Costa et al., 2016). Thus, while the equatorial Pacific is responsible for significant glacial respired carbon storage, it is not the conduit through which carbon was sequestered into the deep ocean and we point to changes in the high latitude Southern Ocean as the principal cause of changes in the Pacific and global oceans (Anderson et al., 2019; Sigman et al., 2010; Jaccard et al., 2016; Rae and Broecker, 2018).

During the last glacial period, where our compilation of aU, $\Delta\delta^{13}C$ and biomarker preservation proxies reaches a critical mass, it is evident that the entire deep Pacific below 1 km, likely at all depths below the eastern tropical Pacific oxygen minimum zone (800 m) (Jaccard and Galbraith, 2012), had lower dissolved oxygen concentrations and higher respired carbon contents than at present. This is an important conclusion because it traces glacial changes to both LCDW and NPDW, expanding the volume of the global ocean to which respired carbon storage can be attributed, in agreement with South Pacific data on LCDW redox state (Wagner and Hendy, 2017). Because we interpret our $\Delta\delta^{13}C$ compilation as placing an upper-most bound on BWO concentrations (38 $\mu mol\ kg^{-1}$ at most, using the last glacial data from TR163-25) we agree with the conservative biomarker preservation-based estimates of BWO (35 $\mu mol\ kg^{-1}$) from Anderson et al. (2019) based on a threshold response of alkenone preservation to BWO. For illustrative purposes, we adopt the extrapolation of Anderson et al. (2019) and suggest that if the changes observed in the deep Pacific are representative of even just half of the glacial ocean's volume, respiratory CO_2 storage could have been ~850 PgC greater than today. This calculation is similar to those proposed by other authors using independent estimates (Jaccard et al., 2009; Sarnthein et al., 2013; Schmittner and Somes, 2016; Skinner et al., 2015) and is sufficient to account for estimates of glacial atmospheric CO_2 drawdown, including losses from the terrestrial biosphere. Our coverage of water masses in the Pacific (Fig. 1) gives us confidence

in our conclusions about lower BWO at water masses sampled by our study sites, but similar compilations are needed to confirm the extent of similar conditions in the Atlantic and other ocean basins.

During the last deglaciation, Southern Ocean records of aU and redox-sensitive Mn have been interpreted as showing two pulses of increased ventilation, one in association with Heinrich Stadial 1 (HS1) and the second in association with the Younger Dryas (YD) (Jaccard et al., 2016). Using the record of Antarctic dust flux (Fig. 12F), which shows dramatically declining dust delivery at the onset of HS1 (Lambert et al., 2008) (17.5 ka), Jaccard and co-authors argued that the first of these deglacial pulses was the most critical for weakening the biological pump and that the second was dominated by an increase in young, oxygenated Antarctic Bottom Water (AABW) relative to Circumpolar Deep Water (CDW) (Jaccard et al., 2016). Both of these deglacial steps in oxygen would have influenced downstream equatorial Pacific water masses, as seen in ^{14}C ventilation ages (Fig. 8E), although their appearance in BWO proxy records would be lagged according to the timescale of ventilation and may have been counterbalanced early on by the influence of warming deep waters on oxygen solubility (Jaccard and Galbraith, 2012). Unfortunately, the two-step structure of this transition is not easily identifiable in any of the cores included in our compilation. Furthermore, the coincidence of increasing equatorial Pacific productivity during deglaciation with greater bottom water ventilation makes determining the exact onset and temporal structure of bottom water re-oxygenation in the Pacific difficult. However, surface productivity and deep water mass ventilation are not unrelated phenomena, with the deglacial decline of nutrient utilization in the Subantarctic Zone (SAZ) of the Southern Ocean being conveyed to the equatorial Pacific thermocline via the influence of Subantarctic Mode Water on the Equatorial Undercurrent (Sarmiento et al., 2004). A record of surface-ocean pH change ($\delta^{11}B$, Fig. 12D) from ODP Site 1238 in the equatorial Pacific (Martínez-Botí et al., 2015) shows the upwelling of respired carbon at the site as early as 21 ka with major deglacial pulses commencing approximately coincident with HS1 and the YD confirming that the surface ocean in the equatorial Pacific was likely one conduit through which the abyssal carbon escaped to the atmosphere (Fig. 12).

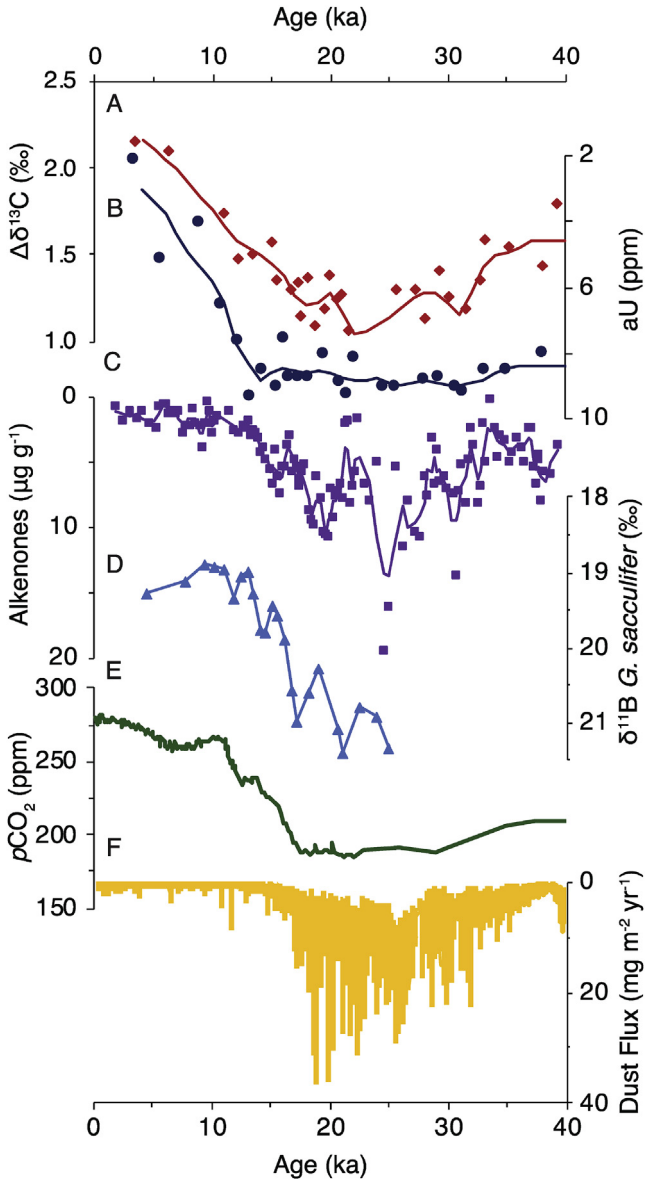

Fig. 12. Global Paleoclimate Indicators. A) $\Delta\delta^{13}C$ (red diamonds and line) from ODP Site 1240 (this study). B) aU (navy blue circles and line) from ODP Site 1240 (this study). C) Alkenone concentrations (purple squares and line) from ODP Site 1240 (Calvo et al., 2011). D) $\delta^{11}B$ of *G. sacculifer* (light blue triangles and line) from ODP Site 1238 (equatorial Pacific) (Martínez-Botí et al., 2015). E) Atmospheric pCO_2 (green line) (Lüthi et al., 2008). F) Antarctic dust flux (orange line) (note inverted y-axis) (Lambert et al., 2008).

In using paleoceanographic data to reconstruct BWO concentrations, our study provides a useful comparison to a recent modeling paper on glacial carbon storage. Khatiwala et al. (2019), argue that the primary cause of glacial carbon drawdown was enhanced air-sea CO_2 disequilibrium driven by increased physical stratification and action of the soft-tissue biological pump. While their estimate of deep ocean carbon storage (856 PgC) is virtually identical to that of Anderson and co-authors (2019), their model underestimates the magnitude of oxygen depletion relative to the observational constraints summarized here (their Fig. S10). While air-sea disequilibrium is an important mechanism of glacial CO_2 drawdown (Eggleston and Galbraith, 2018), the mismatch between reconstructions of BWO and the predictions of Khatiwala et al. suggests that their model overestimates air-sea disequilibrium and underestimates the significance of enhancements to the efficiency of the soft-tissue biological pump related directly to organic carbon export. In recognizing that changes to the magnitude of LGM air-sea disequilibrium were likely important, we point out that the BWO-based respired carbon storage estimate represents a conservative endmember, because it assumes that deep waters were in equilibrium with the atmosphere at the time of formation. If, instead, bottom waters were formed out of equilibrium, with lower dissolved O_2 and higher CO_2 concentrations than assumed, then carbon storage estimated using apparent oxygen utilization would be too low (see discussion in Anderson et al., 2019 and Ito and Follows, 2013). Better estimates of the magnitude of air-sea disequilibrium at the sites of bottom water formation -even modern estimates range from 4 to 35% (A. L. Gordon and Huber, 1990; Rae and Broecker, 2018)- will help to improve future estimates of LGM respired carbon storage, almost certainly revising early estimates upwards.

The early (80–90 ka) onset of low BWO, and the O_2-based estimates of respired carbon storage are of particular significance to the hypothesis that a 'significant release of hydrothermal fluids' contributed to the deglacial rise in atmospheric pCO_2 (Stott et al., 2009, 2019; Stott and Timmermann, 2011). We strongly disagree with this hypothesis for two reasons. First, the synchronous rise in SAZ productivity and oxygen depletion in the Southern Ocean (Jaccard et al., 2016), in tandem with the rise of oxygen depletion observed across the entire abyssal Pacific (*e.g.*: this study, Jaccard

et al., 2016; Jaccard and Galbraith, 2013), is indicative of a long-term sequestration of respired carbon into the deep ocean and is very difficult to attribute to isolated hydrothermal input, including those driven by deglacial changes in sea level (Lund et al., 2016) or temperature (Stott and Timmermann, 2011). Second, the estimated magnitude of carbon storage that can be attributed to the respiratory conversion of sinking organic carbon leaves little room for significant hydrothermal input. We agree that hydrothermal input of radiocarbon-dead hydrothermal CO_2 may have played a role in the marine and atmospheric $\Delta^{14}C$ anomalies observed during the deglacial "Mystery Interval" (Broecker and Barker, 2007), but argue that the primary source of the deglacial CO_2 rise was the venting of respired carbon from the abyssal ocean.

Our new compilation also has bearing on the hypothesis that deep water was formed in the North Pacific during the last glacial termination, specifically during HS1 (*e.g.*: Okazaki et al., 2010). Authigenic uranium data from 2.4 km in the North Pacific (Jaccard and Galbraith, 2013) were previously interpreted as indicating that no young, well-oxygenated water mass could have reached that depth during HS1. This evidence was questioned by Rae et al. (2014) who attributed the observation of continuous aU deposition from the LGM through ~15 ka and the onset of the Bølling Allerød (BA) to insufficient time for oxygen penetration during HS1 and/or resumption of oxygen limitation during the BA and downcore signal migration. In light of the sedimentation rate of this core (RNDB-13 PC at more than 8 cm ka^{-1}) we favor the original interpretation of Jaccard and Galbraith. Data from TR163-25, originally from Hoogakker et al. (2018), provide further support for Jaccard and Galbraith's argument for "expanded North Pacific intermediate water" rather than NPDW formation. This core shows that equatorial Pacific BWO remained below 50 μmol kg^{-1} at 2.7 km through 15 ka. Recalling that $\Delta\delta^{13}C$ data are not subject to the same burndown effects as aU, and that BWO estimates derived from $\Delta\delta^{13}C$ are upper estimates, core TR163-25 can be used to place an upper estimate on BWO concentrations at 15 ka. Data from TR163-25 do not reflect the influence of a young, well-oxygenated water mass during the deglaciation, but rather old, oxygen-depleted PDW.

6. Avenues for future work

6.1. Remaining questions

The evidence for reduced glacial oxygen levels in LCDW summarized here resolves uncertainty about the extent of respired carbon storage in the equatorial Pacific. While the biomarker preservation data make it clear that glacial oxygen concentrations were lower and as a corollary, respired carbon contents were higher, aU data (more specifically, the lack of preserved aU in LCDW-bathed deep Pacific sites) leaves open the possibility that oxygen concentrations were not as low in LCDW as they were in NPDW. Given the present-day distribution of oxygen in deep Pacific water masses (Fig. 1B), reflecting ventilation at abyssal depths by bottom water formed around Antarctica, it is not surprising that LCDW might have remained better oxygenated than NPDW during glacial periods. Additional data from higher accumulation rate sites bathed by LCDW (for instance on the Peru/Chile margin) may help to constrain this question in the future. For example, new $\Delta\delta^{13}C$ data might be used to provide an upper bound on LCDW oxygen availability during the LGM. Quantitatively constraining the amount of oxygen and respired carbon contained in these water masses will help us close the glacial-interglacial oxygen budget of the deep ocean and serve as important step towards modeling the magnitude of change required of the various carbon 'pumps' connecting the surface and deep ocean.

Given the high value we place on quantitative reconstructions of BWO it is disappointing that our review of the existing data has led us to conclude that none of the three proxies examined here is truly quantitative. All three are useful proxies, and $\Delta\delta^{13}C$ and biomarker preservation may be able to provide upper estimates of BWO, but more work is needed to fully calibrate these proxies. Additional observations of biomarker preservation may improve its ability to be calibrated quantitatively, and $\Delta\delta^{13}C$ may yet be refined by the identification of a means to quantify the contribution of foraminifera denitrification to the $\delta^{13}C$ signal using cell volumes (Glock et al., 2019), pore densities (Glock et al., 2011), or other approaches including those that might account for the influence of sulfate reduction.

6.2. Best practices

A common thread in our review of the aU, $\Delta\delta^{13}C$ and biomarker preservation proxies is the importance of pairing data from each proxy with a site-specific and trustworthy (i.e. diagenesis-resistant) indicator of organic carbon flux. The overarching importance of these paleoproductivity indicators is that they help us to understand how local changes in aerobic carbon respiration lead to a porewater overprint of the basin-wide signals we are most interested in interpreting. Without an organic carbon flux proxy, aU and $\Delta\delta^{13}C$ would at times appear to yield contradictory information about the sense of BWO changes, and changes in biomarker abundance might be interpreted as solely indicative of preservation when the reality is more complex. A thorough review of equatorial Pacific productivity over the last 30 ka (Costa et al., 2017) gives us confidence in our understanding of regional trends, but the site-specific nuances are critical. We therefore propose that paleoproductivity should be reconstructed in tandem with all new BWO and respired carbon reconstructions.

Changing deglacial productivity presents a significant challenge for reconstructing the temporal sequence of BWO changes in the equatorial Pacific, and post-depositional burndown has the potential to further obscure event timing. Because the depth of oxygen penetration into sediments depends on concentration gradients, porosity and other properties, estimating site-specific burndown depths is challenging. Even if we were to identify a record where we did not expect burndown to have contributed to the structure of the record, the deglacial rise in productivity appears to occur roughly between 20 and 7.5 ka (Costa et al., 2017), precisely covering the interval where we would expect changes in BWO to imprint the proxy record, thus confounding our ability to interpret changes as unequivocally indicative of BWO rather than productivity-driven changes in porewater redox state. We therefore propose that equatorial Pacific records of aU, $\Delta\delta^{13}C$ and biomarker preservation are not appropriate for temporal assignments of change in the absence of concerted site-specific efforts to constrain the extent of burndown and the influence of local productivity on BWO. There are other proxies better suited for determining the timing of deglacial respired carbon release (*e.g.*: B/Ca (Rae et al., 2011; Umling and Thunell, 2018; Yu et al., 2010), and $\delta^{11}B$ (Gray et al., 2018; Martínez-Botí et al., 2015)). These approaches do not specifically address BWO, but we contend that combining them with BWO proxies is currently our best hope for understanding the temporal trends of deglacial change in the equatorial Pacific.

Finally, because none of the proxies here is a perfect indicator of BWO alone, we emphasize the importance of multiproxy approaches. Using Site ODP Site 1240 as an example, our net interpretation of proxy change was significantly different using all three BWO indicators, when informed by the Ba_{xs} flux, then it might have been using one record in isolation. Intra-core differences in proxies are clearly exacerbated at sites where sedimentation rates are low or changes in productivity have been high. We thus emphasize the

value of using multiple BWO proxies to reconstruct the histories of sites and regions in the pursuit of answers to paleoceanographic questions regarding ice age storage of carbon in the deep ocean.

7. Conclusions

Our new compilation of bottom water oxygen data from the equatorial Pacific improves our understanding of both proxies and the paleoceanographic records of deep water ventilation and respired carbon storage. We provide insight into the limitations of single-proxy reconstructions using aU, $\Delta\delta^{13}C$, or biomarker-preservation alone, and make a strong case for multi-proxy reconstructions that are informed by site-specific productivity records. Although questions remain about the validity of both $\Delta\delta^{13}C$ and biomarker-preservation as truly quantitative proxies, we have provided evidence that they provide useful maximum estimates of BWO and minimum estimates of glacial carbon storage. Our interpretation of equatorial Pacific BWO records and extrapolation of these data to the broader Pacific basin support evidence for the deglacial transfer of ~850 Pg of C from the abyssal ocean to the atmosphere, and likely identifies the primary source of the deglacial rise in atmospheric CO_2. In identifying data in support of reduced oxygen concentrations in all deep Pacific Ocean water masses below 1 km we argue that glacial carbon storage was enhanced in both NPDW and LCDW but leave open questions about the partitioning of carbon between those reservoirs. Our redox data provide strong evidence that the water mass sources of deglacial CO_2 were old and oxygen-depleted, and had likely last communicated with the atmosphere in the Southern Ocean, not the North Pacific. Questions remain about the precise quantification of oxygen and carbon in the abyssal Pacific, and the relative role of other water masses in glacial carbon storage, but using the best practices recommended here we are confident there is still progress to be made using the redox proxies in our paleoceanographic toolbox.

Author contribution statement

A.W.J., J.F.M. and R.F.A. designed the research, A.W.J. performed the analyses and constructed the figures. All authors were involved in writing and revising the manuscript.

Data archival

New data supporting the results of this contribution are available through PANGAEA at https://doi.pangaea.de/10.1594/PANGAEA.908245.

Acknowledgements

The authors would like to thank Marty Fleisher and Roseanne Schwartz for assistance in the lab. This manuscript was improved by comments from three anonymous referees. This research was funded in part by an award from the US National Science Foundation (AGS-1502889 to J.F.M. and G.W.), and in part by an award from Rolex and the Explorer's Club to A.W.J. S.L.J. acknowledges support from the Swiss National Science Foundation (grants PP00P2_144811 and PP00P2_172915).

Appendix A. Supplementary data

Supplementary data to this article can be found online at https://doi.org/10.1016/j.quascirev.2019.106065.

References

Allen, K.A., Sikes, E.L., Hönisch, B., Elmore, A.C., Guilderson, T.P., Rosenthal, Y., Anderson, R.F., 2015. Southwest Pacific deep water carbonate chemistry linked to high southern latitude climate and atmospheric CO_2 during the Last. Quat. Sci. Rev. 122, 180–191. https://doi.org/10.1016/j.quascirev.2015.05.007.

Anderson, R.F., 1982. Concentration, vertical flux, and remineralization of particulate uranium in seawater. Geochem. Cosmochim. Acta 46, 1293–1299. https://doi.org/10.1016/0016-7037(82)90013-8.

Anderson, R.F., Sachs, J.P., Fleisher, M.Q., Allen, K.A., Yu, J., Koutavas, A., Jaccard, S.L., 2019. Deep-sea oxygen depletion and ocean carbon sequestration during the last ice age. Glob. Biogeochem. Cycles. https://doi.org/10.1029/2018GB006049.

Archer, D., Winguth, A., Lea, D., Mahowald, N., 2000. What caused the glacial/interglacial atmospheric pCO_2 cycles? Rev. Geophys. 38, 159–189. https://doi.org/10.1029/1999RG000066.

Bereiter, B., Shackleton, S., Baggenstos, D., Kawamura, K., Severinghaus, J., 2018. Mean global ocean temperatures during the last glacial transition. Nature 553, 39–44. https://doi.org/10.1038/nature25152.

Bova, S.C., Herbert, T.D., Altabet, M.A., 2018. Ventilation of northern and southern sources of aged carbon in the eastern equatorial pacific during the younger Dryas rise in atmospheric CO_2. Paleoceanogr. Paleoclimatol. 33, 1151–1168. https://doi.org/10.1029/2018PA003386.

Boyle, E.A., 1990. Quaternary deepwater paleoceanography. Science 249, 863–870. https://doi.org/10.1126/science.249.4971.863.

Bradtmiller, L.I., Anderson, R.F., Fleisher, M.Q., Burckle, L.H., 2006. Diatom productivity in the equatorial Pacific Ocean from the last glacial period to the present: a test of the silicic acid leakage hypothesis. Paleoceanography 21. https://doi.org/10.1029/2006PA001282.

Bradtmiller, L.I., Anderson, R.F., Sachs, J.P., Fleisher, M.Q., 2010. A deeper respired carbon pool in the glacial equatorial Pacific Ocean. Earth Planet. Sci. Lett. 299, 417–425. https://doi.org/10.1016/j.epsl.2010.09.022.

Bradtmiller, L.I., McGee, D., Awalt, M., Evers, J., Yerxa, H., Kinsley, C.W., deMenocal, P.B., 2016. Changes in biological productivity along the northwest African margin over the past 20,000 years. Paleoceanography 31, 185–202. https://doi.org/10.1002/2015PA002862.

Broecker, W., Barker, S., Clark, E., Hajdas, I., Bonani, G., Stott, L., 2004. Ventilation of the glacial deep Pacific Ocean. Science 306, 1169–1172. https://doi.org/10.1126/science.1102293.

Broecker, W., Clark, E., 2011. Radiocarbon-age differences among coexisting planktic foraminifera shells: the Barker Effect. Paleoceanography 26. https://doi.org/10.1029/2011PA002116.

Broecker, W., Clark, E., 2010. Search for a glacial-age ^{14}C-depleted ocean reservoir. Geophys. Res. Lett. 37, L13606. https://doi.org/10.1029/2010GL043969.

Broecker, W., Clark, E., Barker, S., 2008. Near constancy of the Pacific Ocean surface to mid-depth radiocarbon-age difference over the last 20 kyr. Earth Planet. Sci. Lett. 274, 322–326. https://doi.org/10.1016/j.epsl.2008.07.035.

Broecker, W.S., Barker, S., 2007. A 190‰ drop in atmosphere's $\Delta^{14}C$ during the 'Mystery Interval' (17.5 to 14.5 kyr). Earth Planet. Sci. Lett. 256, 90–99. https://doi.org/10.1016/j.epsl.2007.01.015.

Broecker, W.S., Peng, T.H., 1974. Gas exchange rates between air and seasea. Tellus 26, 21–35. https://doi.org/10.1111/j.2153-3490.1974.tb01948.x.

Calvo, E., Pelejero, C., Pena, L.D., Cacho, I., Logan, G.A., 2011. Eastern Equatorial Pacific Productivity and related-CO_2 Changes since the Last Glacial Period 108, pp. 5537–5541. https://doi.org/10.1073/pnas.1009761108.

Colley, S., Thomson, J., 1985. Recurrent uranium relocations in distal turbidites emplaced in pelagic conditions. Quat. Sci. Rev. 49, 2339–2348. https://doi.org/10.1016/0016-7037(85)90234-0.

Colley, S., Thomson, J., Toole, J., 1989. Uranium relocations and derivation of quasi-isochrons for a turbidite/pelagic sequence in the Northeast Atlantic. Quat. Sci. Rev. 53, 1223–1234. https://doi.org/10.1016/0016-7037(89)90058-6.

Costa, K.M., Jacobel, A.W., McManus, J.F., Anderson, R.F., Winckler, G., Thiagarajan, N., 2017. Productivity patterns in the equatorial Pacific over the last 30,000 years. Glob. Biogeochem. Cycles 31, 850–865. https://doi.org/10.1002/2016GB005579.

Costa, K.M., McManus, J.F., Anderson, R.F., Ren, H., Sigman, D.M., Winckler, G., Fleisher, M.Q., Marcantonio, F., Ravelo, A.C., 2016. No iron fertilization in the equatorial Pacific Ocean during the last ice age. Nature 529, 519–522. https://doi.org/10.1038/nature16453.

Cowie, G., Mowbray, S., Kurian, S., Sarkar, A., White, C., Anderson, A., Vergnaud, B., Johnstone, G., Brear, S., Woulds, C., Naqvi, S.W.A., Kitazato, H., 2014. Comparative organic geochemistry of Indian margin (Arabian Sea) sediments: estuary to continental slope. Biogeosciences 11, 6683–6696. https://doi.org/10.5194/bg-11-6683-2014.

Crusius, J., Thomson, J., 2000. Comparative behavior of authigenic Re, U, and Mo during reoxidation and subsequent long-term burial in marine sediments. Geochem. Cosmochim. Acta 64, 2233–2242. https://doi.org/10.1016/S0016-7037(99)00433-0.

de la Fuente, M., Skinner, L., Calvo, E., Pelejero, C., Cacho, I., 2015. Increased reservoir ages and poorly ventilated deep waters inferred in the glacial Eastern Equatorial Pacific. Nat. Commun. 6 https://doi.org/10.1038/ncomms8420.

De Lange, G.J., 1998. Oxic vs. anoxic diagenetic alteration of turbiditic sediments in the Madeira Abyssal Plain, eastern North Atlantic. Proc. Ocean Drill. Program Sci. Results 157.

De Lange, G.J., 1986. Early diagenetic reactions in interbedded pelagic and turbiditic

sediments in the Nares Abyssal Plain (western North Atlantic): consequences for the composition of sediment and interstitial water. Geochem. Cosmochim. Acta 50, 2543–2561.
Dong, W., Brooks, S.C., 2006. Determination of the formation constants of ternary complexes of uranyl and carbonate with alkaline Earth metals (Mg^{2+}, Ca^{2+}, Sr^{2+}, and Ba^{2+}) using anion exchange method. Environ. Sci. Technol. 40, 4689–4695. https://doi.org/10.1021/es0606327.
Drexler, J.W., Rose, W.I., Sparks, R.S.J., Ledbetter, M.T., 1980. The Los Chocoyos ash, Guatemala: a major stratigraphic marker in Middle America and in three ocean basins. Quat. Res. 13, 327–345. https://doi.org/10.1016/0033-5894(80)90061-7.
Duchamp-Alphonse, S., Giuseppe, S., Michel, E., Beaufort, L., Gally, Y., Jaccard, S.L., 2018. Enhanced ocean-atmosphere carbon partitioning via the carbonate counter pump during the last deglacial. Nat. Commun. 9 (1), 2396. https://doi.org/10.1038/s41467-018-04625-7.
Eggleston, S., Galbraith, E.D., 2018. The devil's in the disequilibrium: multi-component analysis of dissolved carbon and oxygen changes under a broad range of forcings in a general circulation model. Biogeosciences 15, 3761–3777. https://doi.org/10.5194/bg-15-3761-2018.
Endrizzi, F., Rao, L., 2014. Chemical speciation of uranium(VI) in marine environments: complexation of calcium and magnesium ions with $[(UO_2)(CO_3)_3]^{4-}$ and the effect on the extraction of uranium from seawater. Chem. Eur J. 20, 14499–14506. https://doi.org/10.1002/chem.201403262.
Finneran, K.T., Anderson, R.T., Nevin, K.P., Lovley, D.R., 2002. Potential for bioremediation of uranium-contaminated aquifers with microbial U(VI) reduction. Soil Sediment Contam. 11, 339–357. https://doi.org/10.1080/20025891106781.
Fleisher, M.Q., Anderson, R.F., 2003. Assessing the collection efficiency of Ross Sea sediment traps using ^{230}Th and ^{231}Pa. Deep Sea Res. Part II Top. Stud. Oceanogr. 50, 693–712. https://doi.org/10.1016/S0967-0645(02)00591-X.
Francois, R., Altabet, M.A., Yu, E.F., Sigman, D.M., Bacon, M.P., Frank, M., Bohrmann, G., Bareille, G., Labeyrie, L.D., 1997. Contribution of Southern Ocean surface-water stratification to low atmospheric CO_2 concentrations during the last glacial period. Nature 389, 929–935. https://doi.org/10.1038/40073.
François, R., Frank, M., Rutgers van der Loeff, M.M., Bacon, M.P., 2004. ^{230}Th normalization: an essential tool for interpreting sedimentary fluxes during the late Quaternary. Paleoceanography 19. https://doi.org/10.1029/2003PA000939.
François, R., Honjo, S., Manganini, S.J., Ravizza, G.E., 1995. Biogenic barium fluxes to the deep sea: implications for paleoproductivity reconstruction. Glob. Biogeochem. Cycles 9, 289–303. https://doi.org/10.1029/95GB00021.
Glock, N., Eisenhauer, A., Milker, Y., Liebetrau, V., Schonfeld, J., Mallon, J., Sommer, S., Hensen, C., 2011. Environmental influences on the pore density in *Bolivina spissa*. J. Foraminifer. Res. 41, 22–32.
Glock, N., Roy, A.-S., Romero, D., Wein, T., Weissenbach, J., Revsbech, N.P., Høgslund, S., Clemens, D., Sommer, S., Dagan, T., 2019. Metabolic preference of nitrate over oxygen as an electron acceptor in foraminifera from the Peruvian oxygen minimum zone. Proc. Natl. Acad. Sci. 116, 2860–2865. https://doi.org/10.1073/pnas.1813887116.
Glock, N., Schönfeld, J., Eisenhauer, A., Hensen, C., Mallon, J., Sommer, S., 2013. The role of benthic foraminifera in the benthic nitrogen cycle of the Peruvian oxygen minimum zone. Biogeosciences 10, 4767–4783. https://doi.org/10.5194/bg-10-4767-2013.
Gordon, A.L., Huber, B.A., 1990. Southern Ocean winter mixed layer. J. Geophys. Res.: Biogeosciences 95, 11655–11672. https://doi.org/10.1029/JC095iC07p11655.
Gottschalk, J., Skinner, L.C., Lippold, J., Vogel, H., Frank, N., Jaccard, S.L., Waelbroeck, C., 2016. Biological and physical controls in the Southern Ocean on past millennial-scale atmospheric CO_2 changes. Nat. Commun. 7 https://doi.org/10.1038/ncomms11539.
Gray, W.R., Rae, J.W.B., Wills, R.C.J., Shevenell, A.E., Taylor, Ben, Burke, A., Foster, G.L., Lear, C.H., 2018. Deglacial upwelling, productivity and CO_2 outgassing in the north Pacific Ocean. Nat. Geosci. 14, 1. https://doi.org/10.1038/s41561-018-0108-6.
Hartnett, H.E., Keil, R.G., Hedges, J.I., Devol, A.H., 1998. Influence of oxygen exposure time on organic carbon preservation in continental margin sediments. Nature 391, 572–575. https://doi.org/10.1038/35351.
Hayes, C.T., Anderson, R.F., Fleisher, M.Q., 2011. Opal accumulation rates in the equatorial Pacific and mechanisms of deglaciation. Paleoceanography 26. https://doi.org/10.1029/2010PA002008.
Henderson, G.M., 2003. The U-series toolbox for paleoceanography. Rev. Mineral. Geochem. 52, 493–531. https://doi.org/10.2113/0520493.
Herbert, T.D., 2003. 6.15 - alkenone paleotemperature determinations. In: Holland, H.D., Turekian, K.K. (Eds.), Treatise on Geochemistry, Treatise on Geochemistry. Pergamon, Oxford, pp. 391–432. https://doi.org/10.1016/B0-08-043751-6/06115-6.
Herbert, T.D., Peterson, L.C., Lawrence, K.T., Liu, Z., 2010. Tropical ocean temperatures over the past 3.5 million years. Science 328, 1530–1534. https://doi.org/10.1126/science.1185435.
Hernandez-Sanchez, M.T., Mills, R.A., Planquette, H., Pancost, R.D., Hepburn, L., Salter, I., FitzGeorge-Balfour, T., 2011. Quantifying export production in the Southern Ocean: implications for the Ba_{xs} proxy. Paleoceanography 26 (15), 587. https://doi.org/10.1029/2010PA002111.
Hinrichs, K.U., Schneider, R.R., Muller, P.J., Rullkötter, J., 1999. A biomarker perspective on paleoproductivity variations in two Late Quaternary sediment sections from the Southeast Atlantic Ocean. Org. Geochem. 30, 341–366. https://doi.org/10.1016/S0146-6380(99)00007-8.
Hoogakker, B.A.A., Elderfield, H., Schmiedl, G., McCave, I.N., Rickaby, R.E.M., 2015. Glacial–interglacial changes in bottom-water oxygen content on the Portuguese margin. Nat. Geosci. 8, 40–43. https://doi.org/10.1038/ngeo2317.
Hoogakker, B.A.A., Lu, Z., Umling, N., Jones, L., Zhou, X., Rickaby, R.E.M., Thunell, R., Cartapanis, O., Galbraith, E., 2018. Glacial expansion of oxygen-depleted seawater in the eastern tropical Pacific. Nature 562, 410–413. https://doi.org/10.1038/s41586-018-0589-x.
Hoogakker, B.A.A., Thornalley, D.J.R., Barker, S., 2016. Millennial changes in North Atlantic oxygen concentrations. Biogeosci. Discuss. 12, 12947–12973. https://doi.org/10.5194/bg-13-211-2016.
Høgslund, S., Revsbech, N.P., Cedhagen, T., Nielsen, L.P., Gallardo, V.A., 2008. Denitrification, nitrate turnover, and aerobic respiration by benthic foraminiferans in the oxygen minimum zone off Chile. J. Exp. Mar. Biol. Ecol. 359, 85–91.
Ito, T., Follows, M.J., 2013. Air-sea disequilibrium of carbon dioxide enhances the biological carbon sequestration in the Southern Ocean. Glob. Biogeochem. Cycles 27, 1129–1138. https://doi.org/10.1002/2013GB004682.
Jaccard, S.L., Galbraith, E.D., Sigman, D.M., Haug, G.H., Francois, R., Pedersen, T.F., Dulski, P., Thierstein, H.R., 2009. Subarctic Pacific evidence for a glacial deepening of the oceanic respired carbon pool. Earth Planet. Sci. Lett. 277, 156–165. https://doi.org/10.1016/j.epsl.2008.10.017.
Jaccard, S.L., Galbraith, E.D., 2013. Direct Ventilation of the North Pacific Did Not Reach the Deep Ocean during the Last Deglaciation 40, pp. 199–203. https://doi.org/10.1029/2012GL054118.
Jaccard, S.L., Galbraith, E.D., 2012. Large climate-driven changes of oceanic oxygen concentrations during the last deglaciation. Nat. Geosci. 5, 151–156. https://doi.org/10.1038/ngeo1352.
Jaccard, S.L., Galbraith, E.D., Martínez-García, A., Anderson, R.F., 2016. Covariation of deep Southern Ocean oxygenation and atmospheric CO_2 through the last ice age. Nature 530, 207–210. https://doi.org/10.1038/nature16514.
Jaccard, S.L., Hayes, C.T., Martinez-Garcia, A., Hodell, D.A., Anderson, R.F., Sigman, D.M., Haug, G.H., 2013. Two modes of change in Southern Ocean productivity over the past million years. Science 339, 1419–1423. https://doi.org/10.1126/science.1227545.
Jacobel, A.W., Anderson, R.F., Winckler, G., Costa, K.M., Gottschalk, J., Middleton, J.L., Pavia, F.J., Shoenfelt, E.M., Zhou, Y., 2019. No evidence for equatorial Pacific dust fertilization. Nat. Geosci. 12, 154–155. https://doi.org/10.1038/s41561-019-0304-z.
Jacobel, A.W., McManus, J.F., Anderson, R.F., Winckler, G., 2017. Repeated Storage of Respired Carbon in the Equatorial Pacific Ocean over the Last Three Glacial Cycles, vol. 8, p. 1727. https://doi.org/10.1038/s41467-017-01938-x.
Keil, R.G., Cowie, G.L., 1999. Organic matter preservation through the oxygen-deficient zone of the NE Arabian Sea as discerned by organic carbon:mineral surface area ratios. Mar. Geol. 161, 13–22. https://doi.org/10.1016/S0025-3227(99)00052-3.
Khatiwala, S., Schmittner, A., Muglia, J., 2019. Air-sea disequilibrium enhances ocean carbon storage during glacial periods. Sci. Adv. 5, eaaw4981 https://doi.org/10.1126/sciadv.aaw4981.
Kienast, S.S., Kienast, M., Mix, A.C., Calvert, S.E., François, R., 2007. Thorium-230 normalized particle flux and sediment focusing in the Panama Basin region during the last 30,000 years. Paleoceanography 22, PA2213. https://doi.org/10.1029/2006PA001357.
Klinkhammer, G.P., Palmer, M.R., 1991. Uranium in the oceans: where it goes and why. Earth Planet. Sci. Lett. 55, 1799–1806. https://doi.org/10.1016/0016-7037(91)90024-Y.
Koho, K.A., Nierop, K.G.J., Moodley, L., Middelburg, J.J., Pozzato, L., Soetaert, K., Plicht, J.V.D., Reichart, G.J., 2013. Microbial bioavailability regulates organic matter preservation in marine sediments. Biogeosciences 10, 1131–1141. https://doi.org/10.5194/bg-10-1131-2013.
Koutavas, A., Sachs, J.P., 2008. Northern timing of deglaciation in the eastern equatorial Pacific from alkenone paleothermometry. Paleoceanography 23. https://doi.org/10.1029/2008PA001593.
Lambert, F., Delmonte, B., Petit, J.R., Bigler, M., Kaufmann, P.R., Hutterli, M.A., Stocker, T.F., Ruth, U., Steffensen, J.P., Maggi, V., 2008. Dust-climate couplings over the past 800,000 years from the EPICA Dome C ice core. Nature 452, 616–619. https://doi.org/10.1038/nature06763.
Leinen, M., Cwienk, D., Heath, G.R., Biscaye, P.E., Kolla, V., Thiede, J., Dauphin, J.P., 1986. Distribution of biogenic silica and quartz in recent deep-sea sediments. Geology 14, 199–203. https://doi.org/10.1130/0091-7613(1986)14<199:DOBSAQ>2.0.CO;2.
Lengger, S.K., Hopmans, E.C., Sinninghe Damsté, J.S., Schouten, S., 2014. Impact of sedimentary degradation and deep water column production on GDGT abundance and distribution in surface sediments in the Arabian Sea: implications for the TEX86 paleothermometer. Geochem. Cosmochim. Acta 142, 386–399. https://doi.org/10.1016/j.gca.2014.07.013.
Lisiecki, L.E., Raymo, M.E., 2005. A Pliocene-Pleistocene stack of 57 globally distributed benthic δ^{18}O records. Paleoceanography 20. https://doi.org/10.1029/2004PA001071.
Loveley, M.R., Marcantonio, F., Wisler, M.M., Hertzberg, J.E., Schmidt, M.W., Lyle, M., 2017. Millennial-scale iron fertilization of the eastern equatorial Pacific over the past 100,000 years. Nat. Geosci. 22, 1. https://doi.org/10.1038/ngeo3024.
Lund, D.C., Asimow, P.D., Farley, K.A., Rooney, T.O., Seeley, E., Jackson, E.W., Durham, Z.M., 2016. Enhanced East Pacific Rise hydrothermal activity during the last two glacial terminations. Science 351, 478–482. https://doi.org/10.1126/science.aad4296.
Lüthi, D., Le Floch, M., Bereiter, B., Blunier, T., Barnola, J.-M., Siegenthaler, U., Raynaud, D., Jouzel, J., Fischer, H., Kawamura, K., Stocker, T.F., 2008. High-resolution carbon dioxide concentration record 650,000–800,000 years before

present. Nature 453, 379–382. https://doi.org/10.1038/nature06949.
Mackensen, A., Licari, L., 2003. Carbon isotopes of live benthic foraminifera from the South Atlantic: Sensitivity to bottom water carbonate saturation state and organic matter rain rates. The South Atlantic in the Late Quaternary: Reconstruction of Material Budgets and Current Systems. Springer, Berlin, pp. 623–644.
Mangini, A., Jung, M., Laukenmann, S., 2001. What do we learn from peaks of uranium and of manganese in deep sea sediments? Mar. Geol. 177, 63–78. https://doi.org/10.1016/S0025-3227(01)00124-4.
Martínez-Botí, M.A., Marino, G., Foster, G.L., Ziveri, P., Henehan, M.J., Rae, J.W.B., Mortyn, P.G., Vance, D., 2015. Boron isotope evidence for oceanic carbon dioxide leakage during the last deglaciation. Nature 518, 219–222. https://doi.org/10.1038/nature14155.
Martínez-García, A., Sigman, D.M., Ren, H., Anderson, R.F., Straub, M., Hodell, D.A., Jaccard, S.L., Eglinton, T.I., Haug, G.H., 2014. Iron fertilization of the subantarctic ocean during the last ice age. Science 343, 1347–1350. https://doi.org/10.1126/science.1246848.
Mayer, L., Pisias, N.G., Janecek, T., 1992. Ocean drilling program initial reports volume 138. Proc. Ocean Drill. Program Sci. Results 138, 1–8.
McCorkle, D.C., Emerson, S.R., Quay, P.D., 1985. Stable carbon isotopes in marine porewaters. Earth Planet. Sci. Lett. 74, 13–26. https://doi.org/10.1016/0012-821X(85)90162-1.
McCorkle, D.C., Corliss, B.H., Farnham, C.A., 1997. Vertical distributions and stable isotopic compositions of live (stained) benthic foraminifera from the North Carolina and California continental margins. Deep Sea Res. I 44 (6), 983–1024. https://doi.org/10.1016/S0967-0637(97)00004-6.
McCorkle, D.C., Emerson, S.R., 1988. The relationship between pore water carbon isotopic composition and bottom water oxygen concentration. Geochem. Cosmochim. Acta 52, 1169–1178. https://doi.org/10.1016/0016-7037(88)90270-0.
McCorkle, D.C., Keigwin, L.D., Corliss, B.H., Emerson, S.R., 1990. The influence of microhabitats on the carbon isotopic composition of deep-sea benthic foraminifera. Paleoceanography 5 (2), 161–185. https://doi.org/10.1029/PA005i002p00161.
McManus, J., Berelson, W.M., Klinkhammer, G.P., Hammond, D.E., Holm, C., 2005. Authigenic uranium: relationship to oxygen penetration depth and organic carbon rain. Geochem. Cosmochim. Acta 69, 95–108. https://doi.org/10.1016/j.gca.2004.06.023.
Mekik, F., 2014. Radiocarbon dating of planktonic foraminifer shells: a cautionary tale. Paleoceanography 29, 13–29. https://doi.org/10.1002/2013PA002532.
Mix, A.C., Le, J., Shackleton, N.J., 1995. Benthic foraminiferal stable isotope stratigraphy of site 846: 0-1.8 ma. Proc. Ocean Drill. Program Sci. Results 138, 839–854.
Mix, A.C., Tiedemann, R., Blum, P., 2003. Proceedings of the ocean drilling program. Ocean Drill. Program. https://doi.org/10.2973/odp.proc.ir.202.2003.
Nomaki, H., Chikaraishi, Y., Tsuchiya, M., Toyofuku, T., Suga, H., Sasaki, Y., Uematsu, K., Tame, A., Ohkouchi, N., 2015. Variation in the nitrogen isotopic composition of amino acids in benthic foraminifera: implications for their adaptation to oxygen-depleted environments. Limnol. Oceanogr. 60, 1906–1916. https://doi.org/10.1002/lno.10140.
Okazaki, Y., Timmermann, A., Menviel, L., Harada, N., Abe-Ouchi, A., Chikamoto, M.O., Mouchet, A., Asahi, H., 2010. Deepwater formation in the north pacific during the last glacial termination. Science 329, 200–204. https://doi.org/10.1126/science.1190612.
Pena, L.D., Cacho, I., Ferretti, P., Hall, M.A., 2008. El Niño-Southern Oscillation-like variability during glacial terminations and interlatitudinal teleconnections. Paleoceanography 23. https://doi.org/10.1029/2008PA001620.
Pichat, S., Abouchami, W., Galer, S.J.G., 2014. Lead isotopes in the eastern equatorial pacific record quaternary migration of the south westerlies. Earth Planet. Sci. Lett. 388, 293–305. https://doi.org/10.1016/j.epsl.2013.11.035.
Piña-Ochoa, E., Høgslund, S., null), E.G., Cedhagen, T., Revsbech, N.P., Nielsen, L.P., Schweizer, M., Jorissen, F.J., Rysgaard, S., Risgaard-Petersen, N., 2010a. Widespread occurrence of nitrate storage and denitrification among Foraminifera and *Gromiida*. Proc. Natl. Acad. Sci. 107, 1148–1153. https://doi.org/10.1073/pnas.0908440107.
Piña-Ochoa, E., Koho, K.A., Geslin, E., Risgaard-Petersen, N., 2010b. Survival and life strategy of the foraminiferan *Globobulimina turgida* through nitrate storage and denitrification. Mar. Ecol. Prog. Ser. 417, 39–49. https://doi.org/10.3354/meps08805.
Prahl, F.G., De Lange, G.J., Lyle, M., Sparrow, M.A., 1989a. Post-depositional stability of long-chain alkenones under contrasting redox conditions. Nature 341, 434–437. https://doi.org/10.1038/341434a0.
Prahl, F.G., Dymond, J., Sparrow, M.A., 2000. Annual biomarker record for export production in the central Arabian Sea. Deep Sea Res. Part II Top. Stud. Oceanogr. 47, 1581–1604. https://doi.org/10.1016/S0967-0645(99)00155-1.
Prahl, F.G., Muehlhausen, L.A., Lyle, M., 1989b. An organic geochemical assessment of oceanographic conditions at Manop Site C over the past 26,000 years. Paleoceanography 4, 495–510. https://doi.org/10.1029/PA004i005p00495.
Rae, J.W.B., Broecker, W., 2018. What fraction of the Pacific and Indian oceans' deep water is formed in the Southern Ocean? Biogeosciences 15, 3779–3794. https://doi.org/10.5194/bg-15-3779-2018.
Rae, J.W.B., Foster, G.L., Schmidt, D.N., Elliott, T., 2011. Boron isotopes and B/Ca in benthic foraminifera: proxies for the deep ocean carbonate system. Earth Planet. Sci. Lett. 302, 403–413. https://doi.org/10.1016/j.epsl.2010.12.034.
Rae, J.W.B., Sarnthein, M., Foster, G.L., Ridgwell, A., Grootes, P.M., Elliott, T., 2014. Deep water formation in the North Pacific and deglacial CO_2 rise. Paleoceanography 29, 645–667. https://doi.org/10.1002/2013PA002570.
Rafter, P.A., Herguera, J.C., Southon, J.R., 2018. Extreme lowering of deglacial seawater radiocarbon content is recorded by both epifaunal and infaunal benthic foraminifera. Clim. Past Discuss. 1–23. https://doi.org/10.5194/cp-2018-75.
Rippert, N., Max, L., Mackensen, A., Cacho, I., Povea, P., Tiedemann, R., 2017. Alternating influence of northern versus southern-sourced water masses on the equatorial pacific subthermocline during the past 240 ka. Paleoceanography 32, 1256–1274. https://doi.org/10.1002/2017PA003133.
Risgaard-Petersen, N., Langezaal, A.M., Ingvardsen, S., Schmid, M.C., Jetten, M.S.M., Camp den, H.J.M.O., Derksen, J.W.M., Piña-Ochoa, E., Eriksson, S.P., Nielsen, L.P., Revsbech, N.P., Cedhagen, T., van der Zwaan, G.J., 2006. Evidence for complete denitrification in a benthic foraminifer. Nature 443, 93–96. https://doi.org/10.1038/nature05070.
Robinson, R.S., Martinez, P., Pena, L.D., Cacho, I., 2009. Nitrogen isotopic evidence for deglacial changes in nutrient supply in the eastern equatorial Pacific. Paleoceanography 24. https://doi.org/10.1029/2008PA001702.
Rodrigo-Gámiz, M., Rampen, S.W., Schouten, S., Sinninghe Damsté, J.S., 2016. The impact of oxic degradation on long chain alkyl diol distributions in Arabian Sea surface sediments. Org. Geochem. 100, 1–9. https://doi.org/10.1016/j.orggeochem.2016.07.003.
Ronge, T.A., Tiedemann, R., Lamy, F., Kohler, P., Alloway, B.V., De Pol-Holz, R., Pahnke, K., Southon, J., Wacker, L., 2016. Radiocarbon constraints on the extent and evolution of the South Pacific glacial carbon pool. Nat. Commun. 7 https://doi.org/10.1038/ncomms11487.
Russell, A.D., Hönisch, B., Spero, H.J., Lea, D.W., 2004. Effects of seawater carbonate ion concentration and temperature on shell U, Mg, and Sr in cultured planktonic foraminifera. Geochem. Cosmochim. Acta 68, 4347–4361. https://doi.org/10.1016/j.gca.2004.03.013.
Sachs, J.P., Anderson, R.F., 2005. Increased productivity in the subantarctic ocean during Heinrich events. Nature 434, 1118–1121. https://doi.org/10.1038/nature03544.
Sarmiento, J.L., Gruber, N., Brzezinski, M.A., Dunne, J.P., 2004. High-latitude controls of thermocline nutrients and low latitude biological productivity. Nature 427, 56–60. https://doi.org/10.1038/nature02127.
Sarnthein, M., Schneider, B., Grootes, P.M., 2013. Peak glacial ^{14}C ventilation ages suggest major draw-down of carbon into the abyssal ocean. Clim. Past 9, 2595–2614. https://doi.org/10.5194/cp-9-2595-2013.
Schlitzer, R., 2016. Ocean Data View. https://odv.awi.de.
Schmiedel, G., Mackensen, A., 2006. Multispecies stable isotopes of benthic foraminifers reveal past changes of organic matter decomposition and deepwater oxygenation in the Arabian Sea. Paleoceanography 21 (4), 2831. https://doi.org/10.1029/2006PA001284.
Schmittner, A., Bostock, H.C., Cartapanis, O., Curry, W.B., Filipsson, H.L., Galbraith, E.D., Gottschalk, J., Herguera, J.C., Hoogakker, B., Jaccard, S.L., Lisiecki, L.E., Lund, D.C., Méndez, G.M., Stieglitz, J.L., Mackensen, A., Michel, E., Mix, A.C., Oppo, D.W., Peterson, C.D., Repschläger, J., Sikes, E.L., Spero, H.J., Waelbroeck, C., 2017. Calibration of the carbon isotope composition ($\delta^{13}C$) of benthic foraminifera. Paleoceanography 32, 512–530. https://doi.org/10.1002/2016PA003072.
Schmittner, A., Somes, C.J., 2016. Complementary constraints from carbon (^{13}C) and nitrogen (^{15}N) isotopes on the glacial ocean's soft- tissue biological pump. Paleoceanography 31, 669–693. https://doi.org/10.1002/2015PA002905.
Shaw, T.J., Sholkovitz, E.R., Klinkhammer, G., 1994. Redox dynamics in the Chesapeake Bay: the effect on sediment/water uranium exchange. Geochem. Cosmochim. Acta 58, 2985–2995. https://doi.org/10.1016/0016-7037(94)90173-2.
Sigman, D.M., Boyle, E.A., 2000. Glacial/interglacial variations in atmospheric carbon dioxide. Nature 407, 859–869. https://doi.org/10.1038/35038000.
Sigman, D.M., Hain, M.P., Haug, G.H., 2010. The polar ocean and glacial cycles in atmospheric CO_2 concentration. Nature 466, 47–55. https://doi.org/10.1038/nature09149.
Sigman, D.M., Jaccard, S.L., Haug, G.H., 2004. Polar ocean stratification in a cold climate. Nature 428, 59–63. https://doi.org/10.1038/nature02357.
Sinninghe Damsté, J.S., Rijpstra, W.I.C., Reichart, G.-J., 2002. The influence of oxic degradation on the sedimentary biomarker record II. Evidence from Arabian Sea sediments. Geochem. Cosmochim. Acta 66, 2737–2754. https://doi.org/10.1016/S0016-7037(02)00865-7.
Skinner, L., McCave, I.N., Carter, L., Fallon, S., Scrivner, A.E., Primeau, F., 2015. Reduced ventilation and enhanced magnitude of the deep Pacific carbon pool during the last glacial period. Earth Planet. Sci. Lett. 411, 45–52. https://doi.org/10.1016/j.epsl.2014.11.024.
Stott, L., Southon, J., Timmermann, A., Koutavas, A., 2009. Radiocarbon age anomaly at intermediate water depth in the Pacific Ocean during the last deglaciation. Paleoceanography 24, PA2223. https://doi.org/10.1029/2008PA001690.
Stott, L., Timmermann, A., 2011. Hypothesized Link between Glacial/Interglacial Atmospheric CO2 Cycles and Storage/Release of CO2-Rich Fluids from Deep-Sea Sediments, Abrupt Climate Change: Mechanisms, Patterns, and Impacts, Geophysical Monograph Series. American Geophysical Union (AGU), Washington, D. C. https://doi.org/10.1029/2010GM001052.
Stott, L.D., Harazin, K., Quintana Krupinski, N.B., 2019. Hydrothermal carbon release to the ocean and atmosphere from the eastern equatorial Pacific during the last glacial termination. Environ. Res. Lett. 14 https://doi.org/10.1088/1748-9326/aafe28.
Studer, A.S., Sigman, D.M., Mart nez-Garc a, A., Benz, V., Winckler, G., Kuhn, G., Esper, O., Lamy, F., Jaccard, S.L., Wacker, L., Oleynik, S., Gersonde, R., Haug, G.H.,

2015. Antarctic Zone nutrient conditions during the last two glacial cycles. Paleoceanography 30, 845–862. https://doi.org/10.1002/2014PA002745.

Suzuki, T., Ishii, M., Aoyama, M., Christian, J.R., Enyo, K., Kwano, T., Key, R.M., Kosugi, N., Kozyr, A., Miller, L.A., Murata, A., Nakano, T., Ono, T., Saino, T., Sasaki, K., Sasano, D., Takatani, Y., Wakita, M., Sabine, C.L., 2013. PACIFICA Data Synthesis Project. Carbon Dioxide Information Analysis Center. Oak Ridge National Laboratory, Oak Ridge, TN. https://doi.org/10.3334/CDIAC/OTG.PACIFICA_NDP092.

Ternois, Y., Kawamura, K., Keigwin, L., Ohkouchi, N., Nakatsuka, T., 2001. A biomarker approach for assessing marine and terrigenous inputs to the sediments of Sea of Okhotsk for the last 27,000 years. Geochem. Cosmochim. Acta 65, 791–802. https://doi.org/10.1016/S0016-7037(00)00598-6.

Theodor, M., Schmiedl, G., Jorissen, F., Mackensen, A., 2016. Stable carbon isotope gradients in benthic foraminifera as proxy for organic carbon fluxes in the Mediterranean Sea. Biogeosciences 13, 6385–6404. https://doi.org/10.5194/bg-13-6385-2016.

Thiagarajan, N., McManus, J.F., 2019. Productivity and sediment focusing in the Eastern Equatorial Pacific during the last 30,000 years. Deep Sea Res. Oceanogr. Res. Pap. https://doi.org/10.1016/j.dsr.2019.03.007.

Thomson, J., Higgs, N.C., Colley, S., 1996. Diagenetic redistributions of redox-sensitive elements in northeast Atlantic glacial/interglacial transition sediments. Earth Planet. Sci. Lett. 139, 365–377. https://doi.org/10.1016/0012-821X(96)00031-3.

Umling, N.E., Thunell, R.C., 2018. Mid-depth respired carbon storage and oxygenation of the eastern equatorial Pacific over the last 25,000 years. Quat. Sci. Rev. 189, 43–56. https://doi.org/10.1016/j.quascirev.2018.04.002.

Venti, N.L., Billups, K., Herbert, T.D., 2017. Paleoproductivity in the northwestern Pacific Ocean during the pliocene-pleistocene climate transition (3.0–1.8 Ma). Paleoceanography 32, 92–103. https://doi.org/10.1002/2016PA002955.

Wagner, M., Hendy, I.L., 2017. Trace metal evidence for a poorly ventilated glacial Southern Ocean. Quat. Sci. Rev. 170, 109–120. https://doi.org/10.1016/j.quascirev.2017.06.014.

Winckler, G., Anderson, R.F., Fleisher, M.Q., McGee, D., Mahowald, N., 2008. Covariant glacial-interglacial dust fluxes in the equatorial pacific and Antarctica. Science 320, 93–96. https://doi.org/10.1126/science.1150595.

Winckler, G., Anderson, R.F., Jaccard, S.L., Marcantonio, F., 2016. Ocean dynamics, not dust, have controlled equatorial Pacific productivity over the past 500,000 years. Proc. Natl. Acad. Sci. 113, 6119–6124. https://doi.org/10.1073/pnas.1600616113.

Yu, J., Broecker, W.S., Elderfield, H., Jin, Z., McManus, J., Zhang, F., 2010. Loss of carbon from the deep sea since the last glacial maximum. Science 330, 1084–1087. https://doi.org/10.1126/science.1193221.

Zhao, N., Keigwin, L.D., 2018. An atmospheric chronology for the glacial-deglacial Eastern Equatorial Pacific. Nat. Commun. 9, 3077. https://doi.org/10.1038/s41467-018-05574-x.

Zheng, Y., Anderson, R.F., van Geen, A., Fleisher, M.Q., 2002a. Preservation of particulate non-lithogenic uranium in marine sediments. Geochem. Cosmochim. Acta 66, 3085–3092. https://doi.org/10.1016/S0016-7037(01)00632-9.

Zheng, Y., Anderson, R.F., van Geen, A., Fleisher, M.Q., 2002b. Remobilization of authigenic uranium in marine sediments by bioturbation. Geochem. Cosmochim. Acta 66, 1759–1772. https://doi.org/10.1016/S0016-7037(01)00886-9.